

# Kinetic Langevin Splitting Schemes for Constrained Sampling

Neil K. Chada\*    Lu Yu†

March 25, 2026

## Abstract

Constrained sampling is an important and challenging task in computational statistics, concerned with generating samples from a distribution under certain constraints. There are numerous types of algorithm aimed at this task, ranging from general Markov chain Monte Carlo, to unadjusted Langevin methods. In this article we propose a series of new sampling algorithms based on the latter of these, specifically the kinetic Langevin dynamics. Our series of algorithms are motivated on advanced numerical methods which are splitting order schemes, which include the BU and BAO families of splitting schemes. Their advantage lies in the fact that they have favorable strong order (bias) rates and computationally efficiency. In particular we provide a number of theoretical insights which include a Wasserstein contraction and convergence results. We are able to demonstrate favorable results, such as improved complexity bounds over existing non-splitting methodologies. Our results are verified through numerical experiments on a range of models with constraints, which include a toy example and Bayesian linear regression.

**Keywords:** Constrained sampling, Splitting schemes, Unadjusted Langevin algorithms, Wasserstein complexity

## Contents

|          |   |           |
|----------|---|-----------|
| <b>1</b> | <b>Introduction</b>                           | <b>2</b>  |
| 1.1      | Family of Splitting Schemes . . . . .         | 3         |
| 1.2      | Other Related Works . . . . .                 | 5         |
| 1.3      | Contributions . . . . .                       | 5         |
| 1.4      | Outline . . . . .                             | 6         |
| 1.5      | Notation . . . . .                            | 6         |
| <b>2</b> | <b>Background Material &amp; Algorithms</b>   | <b>6</b>  |
| 2.1      | Constrained Splitting Schemes . . . . .       | 8         |
| 2.2      | Extension to Stochastic Gradients . . . . .   | 9         |
| 2.3      | Convergence in Wasserstein Distance . . . . . | 10        |
| <b>3</b> | <b>Main Results</b>                           | <b>11</b> |
| 3.1      | Convergence Analysis of CUBU . . . . .        | 11        |
| 3.1.1    | Extension to SG-CUBU . . . . .                | 12        |
| 3.2      | Convergence Analysis of CBAOAB . . . . .      | 13        |
| 3.2.1    | Extension to SG-CBAOAB . . . . .              | 13        |
| 3.3      | Results for SG-CKLMC . . . . .                | 14        |

---

\*Department of Mathematics, City University of Hong Kong, Hong Kong SAR, [neilchada123@gmail.com](mailto:neilchada123@gmail.com)

†Department of Data Science, City University of Hong Kong, Hong Kong SAR, [lu.yu@cityu.edu.hk](mailto:lu.yu@cityu.edu.hk)

|  |           |
|--|-----------|
| <b>4 Numerical Experiments</b>                       | <b>16</b> |
| 4.1 Circular Constraint . . . . .                    | 16        |
| 4.2 Triangular Constraint . . . . .                  | 16        |
| 4.3 Square Constraint . . . . .                      | 17        |
| 4.4 Bayesian Constrained Linear Regression . . . . . | 18        |
| <b>5 Conclusion</b>                                  | <b>20</b> |
| <b>A Proofs of Theorems</b>                          | <b>24</b> |
| A.1 Proofs of convergence for CUBU . . . . .         | 24        |
| A.2 Proofs of convergence for SG-CUBU . . . . .      | 24        |
| A.3 Proofs of convergence for CBAOAB . . . . .       | 25        |
| A.4 Proofs of convergence for SG-CBAOAB . . . . .    | 26        |
| A.5 Proofs of convergence for SG-CKLMC . . . . .     | 33        |
| <b>B Algorithms</b>                                  | <b>35</b> |

# 1 Introduction

Sampling from probability distributions plays a critical role in various fields of science and engineering. Examples of such fields include numerical weather prediction, geophysical sciences, and more recently machine learning, such as generative modelling or Bayesian neural networks [SSDK21, HNPDS21, SDWGM15]. Most of these applications exploit Monte Carlo methodologies for sampling, with limited, or rarely any significant, restrictions. However, in many situations it is of interest to consider sampling with dealing with convex or compact sets, in other words, restricting the sampling to a particular region within the sample space. We will refer to this task as *constrained sampling*, which will be the focus of this work. Many scenarios involve sampling on constrained, or confined, spaces, for example stochastic optimal control and molecular dynamics [CEAMR12, LM15]. In this context, the problem involves sampling from a probability measure (which we often refer to as the target)  $\nu$  on such sets, which are characterized by a density function of the form

$$\nu(\boldsymbol{\theta}) = \frac{e^{-U(\boldsymbol{\theta})}}{\int_{\mathbb{R}^p} e^{-U(\boldsymbol{\theta})} d\boldsymbol{\theta}}, \quad (1.1)$$

where from the equation,  $U(\boldsymbol{\theta})$  takes the form  $U(\boldsymbol{\theta}) = f(\boldsymbol{\theta}) + \ell_{\mathcal{K}}(\boldsymbol{\theta})$ , where  $f(\boldsymbol{\theta})$  represents a potential function and  $\ell_{\mathcal{K}}(\boldsymbol{\theta})$  is an indicator function ensuring the parameters  $\boldsymbol{\theta}$  lies within a convex and compact set  $\mathcal{K} \subset \mathbb{R}^p$ , for  $p \geq 1$ ,

$$\ell_{\mathcal{K}}(\boldsymbol{\theta}) := \begin{cases} +\infty & \text{if } \boldsymbol{\theta} \notin \mathcal{K} \\ 0 & \text{if } \boldsymbol{\theta} \in \mathcal{K}. \end{cases} \quad (1.2)$$

The absence of smoothness in the target distribution  $\nu$  presents significant challenges because sampling algorithms often depend, quite heavily, on the smoothness properties of the target distribution. This is to ensure that one can effectively explore the state space and produce representative samples of the target  $\nu$ . Motivated by this, we consider the approximation for  $\ell_{\mathcal{K}}$  of the form

$$\ell_{\mathcal{K}}^{\lambda}(\boldsymbol{\theta}) := \frac{1}{2\lambda^2} d_{\mathcal{K}}(\boldsymbol{\theta}),$$

where  $\lambda > 0$  is the tuning parameter and  $d_{\mathcal{K}} : \mathbb{R}^p \rightarrow \mathbb{R}_+$  is a distance function that quantifies the distance between  $\boldsymbol{\theta}$  and the constraint set  $\mathcal{K}$ . We will later introduce specific choices for  $d_{\mathcal{K}}$ . Now we define

$$U^{\lambda}(\boldsymbol{\theta}) := f(\boldsymbol{\theta}) + \ell_{\mathcal{K}}^{\lambda}(\boldsymbol{\theta}), \quad (1.3)$$

and the corresponding surrogate target density  $\nu^{\lambda}$  given as

$$\nu^{\lambda}(\boldsymbol{\theta}) := \frac{e^{-U^{\lambda}(\boldsymbol{\theta})}}{\int_{\mathbb{R}^p} e^{-U^{\lambda}(\boldsymbol{\theta}')} d\boldsymbol{\theta}'}. \quad (1.4)$$

Therefore, our task at hand is now to generate samples from the modified target, denoted as  $\nu^\lambda \propto \exp(-U^\lambda)$ , which is designed with constraints through the constrained set  $\mathcal{K}$  and our potential function (1.3). Therefore, we consider sampling from the target density  $\nu^\lambda \propto \exp(-U^\lambda)$ . A popular approach for this task are kinetic Langevin methods. These methods are based on the kinetic Langevin dynamics (KLD) (also referred to as underdamped Langevin dynamics [CCBJ18, DRD20]), is a well-known approach to model the dynamics of molecular systems. It has been heavily utilized in different mathematical areas, which include molecular dynamics, Bayesian statistics, and more recently machine learning. It is defined through two coupled processes  $\{\mathbf{L}_t\}_{t \geq 0}$  and  $\{\mathbf{V}_t\}_{t \geq 0}$  which are the position and the velocity, defined as the following

$$\begin{aligned} d\mathbf{L}_t &= \mathbf{V}_t dt, \\ d\mathbf{V}_t &= -\nabla U(\mathbf{L}_t) dt - \gamma \mathbf{V}_t dt + \sqrt{2\gamma} d\mathbf{W}_t, \end{aligned} \tag{1.5}$$

where  $U : \mathbb{R}^p \rightarrow \mathbb{R}$  is a potential energy function,  $\{\mathbf{W}_t\}_{t \geq 0}$  is a standard  $p$ -dimensional Brownian motion, and  $\gamma > 0$  is a friction coefficient. Under fairly weak assumptions, the unique invariant measure of the process  $\{\mathbf{L}_t, \mathbf{V}_t\}_{t \geq 0}$  is of the form

$$\nu(d\boldsymbol{\vartheta} d\mathbf{v}) \propto \exp\left(-U(\boldsymbol{\vartheta}) - \frac{\|\mathbf{v}\|^2}{2}\right) d\boldsymbol{\vartheta} d\mathbf{v}. \tag{1.6}$$

An alternative to KLD is to use the overdamped Langevin dynamics (OLD), which instead just considers the process  $\{\mathbf{L}_t\}_{t \geq 0}$  given as

$$d\mathbf{L}_t = -\nabla U(\mathbf{L}_t) dt + \sqrt{2\beta^{-1}} d\mathbf{W}_t, \tag{1.7}$$

where  $\beta^{-1} > 0$  is the inverse temperature parameter. We notice we have no friction term within (1.7). The invariant measure associated with (1.7) is defined as

$$\nu(d\boldsymbol{\vartheta}) \propto \exp(-U(\boldsymbol{\vartheta})) d\boldsymbol{\vartheta}.$$

The benefit of using the KLD over the OLD, is that is known to converge faster to its respective invariant measure. In the context of Bayesian sampling, both (1.5) and (1.7) can be used to generate samples from a distribution  $\nu$ . This is achieved by simply setting the potential as the log-posterior, i.e.  $U = \log \nu$ . Recent work has looked at connecting these processes, to well-known optimization procedures. In order to implement such dynamics, doing so with the full-continuous process is challenging, and often impossible. Therefore one must resort to discretization schemes. The most obvious discretization method is the Euler-Maruyama (EM) scheme, however existing results suggest alternative methods, based on the bias, complexity and stability. One such method is the randomized midpoint method (RMM) [SL19]. The RMM has also provided advantages in error tolerance and condition number dependence, demonstrated through applications in machine learning [LJ24, YY25a, KD24]. In the context of constrained sampling, this was used in the work of Yu et al. [YY25b], where they demonstrate sharper approximation analysis, and improved error bounds in terms of Wasserstein distance.

Despite the success of the RMM applied to constrained sampling, there still remains limitations, such as that it uses two gradient evaluations per time-step. Secondly, for a fixed  $\kappa > 0$  it is noted that the RMM has a complexity of order  $\mathcal{O}(\varepsilon^{-2/3} p^{1/3})$ , for dimension  $p > 0$  and  $\varepsilon > 0$ , which can be improved on. Therefore this promotes the use of potentially better schemes achieving improvements in those aspects. For this, we introduce and motivate the use of an alternative series of schemes referred to splitting order schemes.

## 1.1 Family of Splitting Schemes

A popular choice for solving ODEs are splitting schemes, motivated by Gilbert Strang [Str63], where one splits the dynamics into different components and solve them individually. This is possible due to the fact they can be integrated exactly. This also translates to SDEs which include the KLD. We will introduce two family of splitting schemes, (i) the BU splitting family, and (ii) the BAO splitting

family. For the former, this was introduced in [Zap21]. The method is based on splitting the SDE (1.5) as follows

$$\begin{pmatrix} d\boldsymbol{\vartheta} \\ d\mathbf{v} \end{pmatrix} = \underbrace{\begin{pmatrix} 0 \\ -\nabla U(\boldsymbol{\vartheta})dt \end{pmatrix}}_{\mathcal{B}} + \underbrace{\begin{pmatrix} \mathbf{v}dt \\ -\gamma\mathbf{v}dt + \sqrt{2\gamma}d\mathbf{W}_t \end{pmatrix}}_{\mathcal{U}},$$

which can be integrated exactly over a step of size  $h > 0$ . Given  $\gamma > 0$ , let  $\eta = \exp(-\gamma h/2)$ , and for ease of notation, we define the following operators

$$\mathcal{B}(\boldsymbol{\vartheta}, \mathbf{v}, h) = (\boldsymbol{\vartheta}, \mathbf{v} - h\nabla U(\boldsymbol{\vartheta})), \quad (1.8)$$

and

$$\begin{aligned} \mathcal{U}(\boldsymbol{\vartheta}, \mathbf{v}, h/2, \xi^{(1)}, \xi^{(2)}) &= \left( \boldsymbol{\vartheta} + \frac{1-\eta}{\gamma}\mathbf{v} + \sqrt{\frac{2}{\gamma}} \left( \mathcal{Z}^{(1)}(h/2, \xi^{(1)}) - \mathcal{Z}^{(2)}(h/2, \xi^{(1)}, \xi^{(2)}) \right), \right. \\ &\quad \left. \eta\mathbf{v} + \sqrt{2\gamma}\mathcal{Z}^{(2)}(h/2, \xi^{(1)}, \xi^{(2)}) \right), \end{aligned} \quad (1.9)$$

where

$$\begin{aligned} \mathcal{Z}^{(1)}(h/2, \xi^{(1)}) &= \sqrt{\frac{h}{2}}\xi^{(1)}, \\ \mathcal{Z}^{(2)}(h/2, \xi^{(1)}, \xi^{(2)}) &= \sqrt{\frac{1-\eta^2}{2\gamma}} \left( \sqrt{\frac{1-\eta}{1+\eta}} \cdot \frac{4}{\gamma h} \xi^{(1)} + \sqrt{1 - \frac{1-\eta}{1+\eta}} \cdot \frac{4}{\gamma h} \xi^{(2)} \right). \end{aligned} \quad (1.10)$$

The  $\mathcal{B}$  operator indicated here is as given previously, whereas  $\mathcal{U}$  as defined above is the exact solution in the weak sense of the remainder of the dynamics when  $\xi^{(1)}, \xi^{(2)} \sim \mathcal{N}(0, I_p)$  are independent random vectors. Different palindromic orders of composition of  $\mathcal{B}$  and  $\mathcal{U}$  can be taken to define different numerical integrators of kinetic Langevin dynamics, two such methods are BUB, a half step ( $h/2$ ) in  $\mathcal{B}$ , followed by a full step in  $\mathcal{U}$  and a further half step ( $h/2$ ) in  $\mathcal{B}$  and UBU, a half step ( $h/2$ ) in  $\mathcal{U}$  followed by a full ( $h$ )  $\mathcal{B}$  step, followed by a half ( $h/2$ )  $\mathcal{U}$  step.

The Markov kernel for an UBU step with stepsize  $h$  will be denoted by  $P_h$ , which can be described by (1.11) as follows.

$$\begin{aligned} &\left( \xi_{k+1}^{(i)} \right)_{i=1}^4, \quad \xi_{k+1}^{(i)} \sim \mathcal{N}(0_p, I_p) \text{ for all } i = 1, \dots, 4. \\ &(\boldsymbol{\vartheta}_{k+1}, \mathbf{v}_{k+1}) = \mathcal{UBU} \left( \boldsymbol{\vartheta}_k, \mathbf{v}_k, h, \xi_{k+1}^{(1)}, \xi_{k+1}^{(2)}, \xi_{k+1}^{(3)}, \xi_{k+1}^{(4)} \right) \\ &= \mathcal{U} \left( \mathcal{B} \left( \mathcal{U} \left( \boldsymbol{\vartheta}_k, \mathbf{v}_k, h/2, \xi_{k+1}^{(1)}, \xi_{k+1}^{(2)} \right), h \right), h/2, \xi_{k+1}^{(3)}, \xi_{k+1}^{(4)} \right). \end{aligned} \quad (1.11)$$

The UBU scheme was analyzed in [SSZ21], where its advantages lie in that it only requires one gradient evaluation per iteration but has strong error order of two. Furthermore, its stepsize stability analysis, as presented in [CLPW26], is independent of dimension  $p$ .

Other symmetric splitting methods are possible and have been extensively studied in recent years. In particular one of them are BAO splitting schemes. The solution maps corresponding to these parts may be denoted by  $\mathcal{B}$ ,  $\mathcal{A}$ , and  $\mathcal{O}$ , which are defined as

$$\mathcal{B} = (\boldsymbol{\vartheta}, \mathbf{v} - h\nabla U(\boldsymbol{\vartheta})), \quad \mathcal{A} = (\boldsymbol{\vartheta} + h\mathbf{v}, \mathbf{v}), \quad \mathcal{O} = (\boldsymbol{\vartheta}, \eta^2\mathbf{v} + \sqrt{1-\eta^4}\xi), \quad (1.12)$$

where as before  $\eta = \exp(-\gamma h/2)$ . Examples of such schemes in the BAO family include BAOAB, ABOBA and OBABO schemes [LM13, LM15], which have the advantage that they are second order in the weak (sampling bias). The two families can be related through the relationship, breaking the

$$\mathcal{U} = \mathcal{A} + \mathcal{O}.$$

As mentioned, these methods are known to attain a weak order of  $\mathcal{O}(h^2)$ . However, unlike UBU, they do not attain the same rate for the strong error. A contraction and convergence analysis was presented,

for such schemes, in the following [LPW24b, LPW24a], which also includes the extension to stochastic gradients.

Thus far, there has been no connection in understanding splitting schemes for KLD in the context of constrained sampling, which acts as our motivation, in the penalized setting. Before we discuss our contributions of this paper, we provide a brief overview of related work on constrained sampling using various Langevin-based algorithms.

## 1.2 Other Related Works

The notion of constrained sampling can have many different interpretations, depending on the setup and assumptions placed. Our setup, defined briefly thus far through (1.4), is based on a penalized constrained setting first introduced in the work of [GHZ24]. Their motivation arises from penalty methods from continuous optimization, which includes a penalty term for constraint violations. However, this is not the only setup one could consider for constrained settings. A natural, but difficult setting could be to consider manifolds directly, which require sophisticated mathematical methods to effectively sample from the target. Recent work that has considered this, in the context of Langevin dynamics, includes [KLV22, NDBD24]. Some of these works require technical couplings, to ensure one can obtain both Wasserstein convergence and contraction. Furthermore, much of these works are based on accept-reject MCMC algorithms like HMC. Despite the elegance of such proposed work, we consider a more simplified setting which is easier to begin with, before moving to a potential manifold setting in future work. Other such works include [LST24], where the authors develop a confined BAO integrators for Langevin dynamics. It is the first paper aimed at exploiting such splitting schemes in the context of a confined space. However, it differs in that the dynamics are designed to reflect of boundaries, and the information is encoded into each step of the integrator. More recent literature includes that of [DFT+25, CKK24], where these papers consider a different setup, motivated through a primal-dual setting, and which do not include a KLD setting, i.e. only one underlying process  $\{\mathbf{L}_t\}_{t \geq 0}$ .

## 1.3 Contributions

We highlight our contributions of this work through the following points below:

- We introduce new algorithms for the task of constrained sampling based on the task of sampling from (1.1). Specifically we introduce ULA-type algorithms, based on splitting order discretization schemes, namely UBU and BAOAB. As a result our new algorithms we propose for this work include the CUBU and CBAOAB algorithms.
- We develop a step-size stability analysis for each of the new algorithms discussed above. Such an analysis utilizes assumptions on the underlying potential, such as convexity and smoothness assumptions, which we will provide later in within the document.
- We provide a complexity analysis in terms of Wasserstein convergence, which translates to the number of steps to achieve an order of accuracy  $\varepsilon > 0$ . A summary of our complexity bounds are provided in Table 1, which highlight the gains and improvement by using splitting schemes, over traditional discretization schemes. Our results will consider different projection methods, which include the Bregman and Gauge projection.
- To complement the newly developed constrained sampling algorithms, we also provide extensions to the case of stochastic gradients. This will include both SG-CUBU and SG-BAOAB, as well as a non-splitting scheme for comparison, which was not previously derived. These are also presented in Table 1, which also demonstrate favorable complexity over SG-CKLMC, which we also consider and provide proofs, for this work.
- Numerical experiments are provided on a range of problems to demonstrate the performance gains of the constrained splitting schemes. This will include a toy problem, with constraints defined through both a triangle and circle, and a more advanced numerical example of Bayesian logistic regression. For each example we compare our newly developed algorithms to existing ones.

| Algorithm    | Complexity                         | Reference              | Metric | Projection     |
|--------------|------------------------------------|------------------------|--------|----------------|
| CLMC (PULMC) | $\mathcal{O}(\varepsilon^{-7})$    | [GHZ24]                | $W_2$  | Euclidean      |
| CKLMC        | $\mathcal{O}(\varepsilon^{-4})$    | [YY25b]                | $W_2$  | Euclidean      |
| CUBU         | $\mathcal{O}(\varepsilon^{-3})$    | This work, Theorem 3.1 | $W_1$  | Bregman, Gauge |
| CUBU         | $\mathcal{O}(\varepsilon^{-3})$    | This work, Theorem 3.1 | $W_2$  | Bregman, Gauge |
| CBAOAB       | $\mathcal{O}(\varepsilon^{-3})$    | This work, Theorem 3.3 | $W_1$  | Bregman, Gauge |
| CBAOAB       | $\mathcal{O}(\varepsilon^{-3})$    | This work, Theorem 3.3 | $W_2$  | Bregman, Gauge |
| SG-CUBU      | $\mathcal{O}(\varepsilon^{-6})$    | This work, Theorem 3.2 | $W_1$  | Bregman, Gauge |
| SG-CUBU      | $\mathcal{O}(\varepsilon^{-21/2})$ | This work, Theorem 3.2 | $W_2$  | Bregman, Gauge |
| SG-CBAOAB    | $\mathcal{O}(\varepsilon^{-7})$    | This work, Theorem 3.4 | $W_1$  | Bregman, Gauge |
| SG-CBAOAB    | $\mathcal{O}(\varepsilon^{-25/2})$ | This work, Theorem 3.4 | $W_2$  | Bregman, Gauge |
| SG-CKLMC     | $\mathcal{O}(\varepsilon^{-18})$   | This work, Theorem 3.6 | $W_2$  | Bregman, Gauge |

Table 1: Table of comparison between different discretization schemes for constrained KLD, in terms of their complexity. Our improved rates are highlighted in red.

## 1.4 Outline

The outline of this paper is as follows, we will begin with Section 2, which will provide an overview of the material needed for the latter sections. This will include a discussion on assumptions we will use based on the potential and density function, and the introduction of our constrained splitting order schemes. This will lead onto Section 3 where we present our main theoretical findings which include both a step-size stability analysis and Wasserstein complexity bounds. We will defer the proofs to Appendix A. To verify our theoretical results, we will introduce our numerical simulations in Section 4 demonstrating improvements under our new methods, where we conclude our findings in Section 5. We also present our new methods in algorithmic form in Appendix B.

## 1.5 Notation

Denote the  $p$ -dimensional Euclidean space by  $\mathbb{R}^p$ . We use  $\boldsymbol{\theta}$  for deterministic vectors and  $\boldsymbol{\vartheta}$  for random vectors. For symmetric matrices  $\mathbf{A}$  and  $\mathbf{B}$ , we write  $\mathbf{A} \preceq \mathbf{B}$  (or  $\mathbf{B} \succeq \mathbf{A}$ ) if  $\mathbf{B} - \mathbf{A}$  is positive semi-definite. For a measurable function  $f : \mathbb{R}^p \rightarrow \mathbb{R}$  and a set  $\mathcal{K} \subset \mathbb{R}^p$ , define the oscillation  $\text{osc}_{\mathcal{K}}(f) := \sup_{x \in \mathcal{K}} f(x) - \inf_{x \in \mathcal{K}} f(x)$ . For a twice differentiable function  $f$ , we denote its gradient and Hessian by  $\nabla f$  and  $\nabla^2 f$ , respectively.  $\delta_x$  denotes the Dirac measure concentrated at the point  $x$ .

## 2 Background Material & Algorithms

In this section we provide a primer on the necessary background material before discussing our main results. This includes various assumptions required on the potential function, and on the compact set  $\mathcal{K}$ . After-which, we will introduce our new constrained algorithms which we refer to as CUBU and CBAOAB. This will be then be considered for stochastic gradients. All algorithms are expressed in algorithmic form in the appendices.

We begin this section by assuming the convex and compact set  $\mathcal{K}$  satisfies the following assumptions.

**Assumption 2.1.** *Given constants  $0 < r < R < \infty$ , it holds that  $B_2(r) \subset \mathcal{K} \subset B_2(R)$ , where  $B_2(r)$  denotes the Euclidean ball of radius  $r$  centered at the origin.*

Moreover, we impose the following assumption on the functions  $f$  and  $d_{\mathcal{K}}$ .

**Assumption 2.2.** *The function  $f : \mathbb{R}^p \rightarrow \mathbb{R}$  attains its global minimum at the origin.*

**Assumption 2.3.** *There exists some constants  $0 < c_1 \leq c_2$  such that*

$$c_1 \|\boldsymbol{\theta} - \mathbb{P}_{\mathcal{K}}(\boldsymbol{\theta})\|_2^2 \leq d_{\mathcal{K}}(x) \leq c_2 \|\boldsymbol{\theta} - \mathbb{P}_{\mathcal{K}}(\boldsymbol{\theta})\|_2^2,$$

where  $\mathbb{P}_{\mathcal{K}} : \mathbb{R}^p \rightarrow \mathbb{R}^p$  is a projection operator onto set  $\mathcal{K}$ . Moreover,  $d_{\mathcal{K}}(\boldsymbol{\theta}) \geq 0$  for all  $\boldsymbol{\theta} \in \mathbb{R}^p$ , and  $d_{\mathcal{K}}(\boldsymbol{\theta}) = 0$  whenever  $\boldsymbol{\theta} \in \mathcal{K}$ .

Let us briefly discuss each of the above assumptions. Assumption 2.1 is important and has been made in the various works in the area of constrained sampling [BDMP17, GHZ24]. Assumption 2.2 is made to ensure a convergence analysis can be provided, with convexity. Finally Assumption 2.3 is an assumption on the distance function, which ensures the potential  $U^\lambda$  inherits smoothness and strong convexity from  $f$ .

Related to Assumption 2.3, we now introduce two choices of  $\ell_{\mathcal{K}}$ , based on commonly used projection classes, which are the Bregman and the Gauge projection. These projections have been widely used in various machine learning applications, which include clustering and detection of outliers [XNZ08, Gho19]. We state this below.

**Example 2.1** (Bregman projection). Consider the Bregman projection  $\mathbb{P}_{\mathcal{K}}^B : \mathbb{R}^p \rightarrow \mathcal{K}$ , defined as

$$\mathbb{P}_{\mathcal{K}}^B(\boldsymbol{\theta}) := \underset{\boldsymbol{\theta}' \in \mathcal{K}}{\operatorname{argmin}} (\boldsymbol{\theta} - \boldsymbol{\theta}')^\top Q(\boldsymbol{\theta} - \boldsymbol{\theta}'),$$

such that  $Q \in \mathbb{R}^{p \times p}$  is a positive semi-definite symmetric matrix.

**Example 2.2** (Scaling-based projection). Consider the Gauge projection  $\mathbb{P}_{\mathcal{K}}^G : \mathbb{R}^p \rightarrow \mathcal{K}$ , defined as

$$\mathbb{P}_{\mathcal{K}}^G := \frac{\boldsymbol{\theta}}{g_{\mathcal{K}}(\boldsymbol{\theta})},$$

such that  $g_{\mathcal{K}}$  is a variant of the Gauge function, which is associated with the set  $\mathcal{K}$ , given as

$$g_{\mathcal{K}}(\boldsymbol{\theta}) := \inf\{t \geq 1 : \boldsymbol{\theta} \in t\mathcal{K}\}.$$

We remark that the Bregman distance is equivalent to the squared Mahalanobis distance, defined as  $F(\boldsymbol{\theta}) = \frac{1}{2}\boldsymbol{\theta}^\top Q\boldsymbol{\theta}$ . Therefore, we can consider a distance function of the form

$$d_{\mathcal{K}}(\boldsymbol{\theta}) = \|\boldsymbol{\theta} - \mathbb{P}_{\mathcal{K}}^B(\boldsymbol{\theta})\|_2^2.$$

As a result The Bregman projection, can be written as

$$\mathbb{P}_{\mathcal{K}}^B(\boldsymbol{\theta}) = \frac{1}{2\lambda^2} \|\boldsymbol{\theta} - \mathbb{P}_{\mathcal{K}}^B(\boldsymbol{\theta})\|_2^2 = \inf_{\boldsymbol{\theta}' \in \mathbb{R}^p} \left( \ell_{\mathcal{K}}(\boldsymbol{\theta}') + \frac{1}{2\lambda^2} (\boldsymbol{\theta} - \boldsymbol{\theta}')^\top Q(\boldsymbol{\theta} - \boldsymbol{\theta}') \right).$$

Let us now place a number of common, and important, assumptions on  $f$  as well the potential  $U^\lambda$ , which can be found below. These assumptions are crucial for our error analysis, and step-size stability analysis. They are mostly generic assumptions used within the literature of sampling as an optimization procedure [Che25].

**Assumption 2.4.** The function  $f : \mathbb{R}^p \rightarrow \mathbb{R}$  is twice continuously differentiable, and  $m$ -strongly convex, that is,

$$f(\boldsymbol{\theta}') \geq f(\boldsymbol{\theta}) + \langle \nabla f(\boldsymbol{\theta}), \boldsymbol{\theta}' - \boldsymbol{\theta} \rangle + \frac{m}{2} \|\boldsymbol{\theta} - \boldsymbol{\theta}'\|^2.$$

Moreover,  $f$  is  $L$ -smooth, which satisfies the following

$$\|\nabla f(\boldsymbol{\theta}) - \nabla f(\boldsymbol{\theta}')\| \leq L \|\boldsymbol{\theta} - \boldsymbol{\theta}'\|, \quad \forall \boldsymbol{\theta}, \boldsymbol{\theta}' \in \mathbb{R}^p,$$

where  $m > 0$  and  $L > 0$  are the strong convex, and Lipschitz, constants.

As shown in Lemmas 12 and 13 from [YY25b], the surrogate potential  $U^\lambda$  inherits the smoothness and strong convexity of  $f$ , provided that the distance function  $d_{\mathcal{K}}$  satisfies Assumption 2.3. More specifically,  $U^\lambda$  is  $m$ -strongly convex and  $M^\lambda$ -smooth with

$$M^\lambda = L + \frac{1}{\lambda^2} C_{\text{proj}},$$

where the constants  $C_{\text{proj}} > 0$  depends on the specific choice of the projection operator. In this work, we focus on the Bregman projection and the Gauge projection introduced in [YY25b], for which  $C_{\text{proj}}$  can be taken as a universal positive constant. Furthermore, we require that  $U^\lambda$  satisfies the following assumption.

**Assumption 2.5** (Lipschitz Hessian). *Assume both the function  $f : \mathbb{R}^p \rightarrow \mathbb{R}$  and the surrogate potential  $U^\lambda : \mathbb{R}^p \rightarrow \mathbb{R}^p$  are three times differentiable. Suppose there exist constants  $L_1, M_1^\lambda > 0$  such that, for any  $\boldsymbol{\theta} \in \mathbb{R}^p$  and arbitrary  $w_1, w_2 \in \mathbb{R}^p$ ,*

$$\|H_f'(\boldsymbol{\theta})[w_1, w_2]\| \leq L_1 \|w_1\| \|w_2\|, \quad \|H_\lambda'(\boldsymbol{\theta})[w_1, w_2]\| \leq M_1^\lambda \|w_1\| \|w_2\|,$$

where  $H_f : \mathbb{R}^p \rightarrow \mathbb{R}^{p \times p}$  and  $H_\lambda : \mathbb{R}^p \rightarrow \mathbb{R}^{p \times p}$  denotes the Hessian of  $f$  and  $U^\lambda$ , respectively.

We note that the constant  $M_1^\lambda$  depends on the geometry of the constraint set  $\mathcal{K}$ , and the parameter  $\lambda$  enters the bound through  $M_1^\lambda$ . Consider Example 2.1 with  $Q = I$ , which corresponds to the Euclidean projection. In this case, the distance function simplifies to

$$d_{\mathcal{K}}(\boldsymbol{\theta}) = \|\boldsymbol{\theta} - \mathbb{P}_{\mathcal{K}}^B(\boldsymbol{\theta})\|_2^2.$$

**Example 2.3** (Ellipsoid). *Consider the ellipsoidal constraint*

$$\mathcal{K} = \{\boldsymbol{\theta} \in \mathbb{R}^p : \boldsymbol{\theta}^\top A \boldsymbol{\theta} \leq 1\}, \quad A = A^\top \succ 0,$$

where the matrix  $A$  has minimum and maximum eigenvalues denoted by  $\lambda_{\min}$  and  $\lambda_{\max}$ , respectively. Then we have the following constant

$$M_1^\lambda = L_1 + \frac{4}{\lambda^2} \left( \frac{\lambda_{\max}}{\lambda_{\min}} \right)^3.$$

**Example 2.4** ( $\ell_q$ -ball with  $q > 2$ ). *Consider the constraint*

$$\mathcal{K} = \{\boldsymbol{\theta} \in \mathbb{R}^p : \|\boldsymbol{\theta}\|_q \leq 1\}$$

Then we have the following constant

$$M_1^\lambda = L_1 + \frac{8}{\lambda^2} p^{3/2} (q-1)^2.$$

## 2.1 Constrained Splitting Schemes

Let us introduce our first constrained algorithm which we refer to as *constrained-UBU*, or abbreviated to CUBU. The form of the splitting is in the same spirit as UBU [SSZ21], with the key difference of the  $\mathcal{B}$ -operator, which is defined as

$$\mathcal{B}^c(\boldsymbol{\vartheta}, \mathbf{v}, h) = (\boldsymbol{\vartheta}, \mathbf{v} - h \nabla U^\lambda(\boldsymbol{\vartheta})), \quad (2.1)$$

for  $h > 0$ , which includes the potential  $U^\lambda(\boldsymbol{\vartheta})$  given as (1.9), and where the  $\mathcal{U}$  operator remains the same as before, i.e.

$$\begin{aligned} \mathcal{U}(\boldsymbol{\vartheta}, \mathbf{v}, h/2, \xi^{(1)}, \xi^{(2)}) &= \left( \boldsymbol{\vartheta} + \frac{1-\eta}{\gamma} \mathbf{v} + \sqrt{\frac{2}{\gamma}} \left( \mathcal{Z}^{(1)}(h/2, \xi^{(1)}) - \mathcal{Z}^{(2)}(h/2, \xi^{(1)}, \xi^{(2)}) \right), \right. \\ &\quad \left. \eta \mathbf{v} + \sqrt{2\gamma} \mathcal{Z}^{(2)}(h/2, \xi^{(1)}, \xi^{(2)}) \right), \end{aligned}$$

with similar definitions of  $\mathcal{Z}^{(1)}$  and  $\mathcal{Z}^{(2)}$  provided through Eqn. (1.10). The acceleration of UBU requires the surrogate function  $U^\lambda$  to be smooth and strongly convex. This requirement is satisfied under Assumption 2.3, provided that  $f$  is strongly convex and smooth. The bounded third derivative condition, as stated in Assumption 3 of [SSZ21], requires an additional assumption on the boundary of the constraint set  $\mathcal{K}$ . Algorithm 1 in the appendix provides an algorithmic form of the CUBU.

To establish the convergence of UBU under constraints, we need the following results by Theorems 23 and 25 from [SSZ21].

We now extend the existing Wasserstein convergence result of UBU to CUBU, provided below.

**Theorem 2.1.** Under Assumptions 2.4 - 2.5, (Assumption 1-3 in [SSZ21]), and setting  $\gamma = 2$ , it holds for a small  $h > 0$  that

$$W_2(\nu^\lambda, \nu_n^{\text{UBU}}) \leq \left(1 - \frac{mh}{3M^\lambda}\right)^n W_2(\nu^\lambda, \nu_0^{\text{UBU}}) + \left(\frac{1}{\sqrt{M^\lambda}} + C_1 \frac{M_1^\lambda}{(M^\lambda)^2}\right) \kappa \sqrt{p} h^2.$$

where  $C_1$  is a universal constant. The exact notion of Wasserstein convergence, and the  $W_2$  metric will be provided in Section 2.3.

Our final constrained splitting scheme we introduce is the *constrained-BAOAB*, abbreviated to CBAOAB. In this setup, we now modify our original mappings as now

$$\mathcal{B} = (\boldsymbol{\vartheta}, \mathbf{v} - h\nabla U^\lambda(\boldsymbol{\vartheta})), \quad \mathcal{A} = (\boldsymbol{\vartheta} + h\mathbf{v}, \mathbf{v}), \quad \mathcal{O} = (\boldsymbol{\vartheta}, \eta^2\mathbf{v} + \sqrt{1 - \eta^4}\xi), \quad (2.2)$$

for  $\lambda > 0$ , arising from Eqn. (1.3). Algorithm 2 in the appendix provides an algorithmic form of the CBAOAB.

**Remark 2.2.** We remark there are other existing splitting schemes, based on the BAO family for the KLD. These include OBABO and ABOBA. Our reason for considering only BAOAB, is related to its improvement in terms of the weak error (also asymptotic bias), which is of order 2, and that it has no bias when aiming to sample from Gaussian targets. Extending this, provides no additional difficulties but would prolong the paper with very similar tedious calculations. Therefore we consider this for potential future work.

## 2.2 Extension to Stochastic Gradients

For many practical scenarios, the exact computation of the potential can be difficult, or time-consuming, especially for high-dimensions. As a result, we consider the use of stochastic gradients (SG), which instead do not require the full evaluation of  $\nabla U^\lambda(\boldsymbol{\theta})$ . The form of our SG-based methods we consider, are based on the notion of mini-batching. In order to consider SG variants, we require a definition of our inexact gradient, which is given below.

**Definition 2.1.** A stochastic gradient approximation of a potential  $f$  is defined by a function  $\mathcal{G} : \mathbb{R}^p \times \Omega \rightarrow \mathbb{R}^p$  and a probability distribution  $\rho$  on a Polish space  $\Omega$ , such that for every  $\boldsymbol{\theta} \in \mathbb{R}^p$ ,  $\mathcal{G}(\boldsymbol{\theta}, \cdot)$  is measurable on  $(\Omega, \mathcal{F})$ , and for  $\omega \sim \rho$ ,

$$\mathbb{E}(\mathcal{G}(\boldsymbol{\theta}, \omega)) = \nabla f(\boldsymbol{\theta}).$$

The function  $\mathcal{G}$  and the distribution  $\rho$  together define the stochastic gradient, which we denote as  $(\mathcal{G}, \rho)$ .

As we are considering a stochastic gradient, one possibility is to directly add noise to the gradient, which is written as  $(\mathcal{G}, \rho) = \nabla f(\boldsymbol{\theta}) + \xi$ , where  $\xi \sim \mathcal{N}(0, 1)$  is a random normal perturbation. Then, we can place the following assumptions on the stochastic gradient.

**Assumption 2.6.** Let us assume we have a stochastic (or noisy) gradient defined through Definition 2.1, then we have the following assumptions.

- (i)  $(\mathcal{G}, \rho)$  is an unbiased estimate of  $\nabla f(\boldsymbol{\theta})$  (unbiased gradient).
- (ii)  $\mathbb{E} \left[ \left\| (\mathcal{G}, \rho) - \nabla f(\boldsymbol{\theta}) \right\|^2 \middle| \boldsymbol{\theta} \right] \leq \sigma_1^2 L^2 (\|\boldsymbol{\theta}\|^2)$  (bound on the stochastic gradient).
- (iii)  $\mathbb{E} \left[ \left\| \nabla_{\boldsymbol{\theta}} (\mathcal{G}, \rho) - \nabla^2 f(\boldsymbol{\theta}) \right\|^2 \middle| \boldsymbol{\theta} \right] \leq \sigma_2^2$  (bound on the second derivative).

In practice, the potential function  $f$  often takes the form

$$f(\boldsymbol{\theta}) = \sum_{i=1}^n f_i(\boldsymbol{\theta}).$$

Accordingly, the stochastic gradient of  $f$  is typically computed as

$$\tilde{\nabla} f(\boldsymbol{\theta}) = \frac{1}{b} \sum_{j \in \Omega} f_j(\boldsymbol{\theta}),$$

where  $\Omega \subset \{1, \dots, n\}$  is a mini-batch of size  $b$ . In this setting, we have  $\sigma_1^2 = \mathcal{O}(1/b)$  and  $\sigma_2^2 = \mathcal{O}(1/b)$ .

Stochastic gradient versions of BAOAB and UBU have been analyzed, and discussed in a series of works, i.e. [CLPW26, LPW24a], which discuss contraction rates and non-asymptotic convergence in the Wasserstein metric. Later we will use some of these results, to establish similar results in the constrained setting. In our setup, we provide two additional algorithms, the SG-CUBU and SG-BAOAB, which are also provided in Algorithms 1 and 2. We do not state the full algorithms for for the full-gradient versions, to avoid repetition, but follow very similarly.

We briefly remark that Assumption 2.6 contains sub-assumptions that will be specific to different SG algorithms.

### 2.3 Convergence in Wasserstein Distance

In order to verify our error bounds, we require a sufficient metric. We will consider the Wasserstein distance, which is a popular metric to show convergence of sampling algorithms. In particular, we will focus on Wasserstein contraction [EGZ19, Dal17]. The key underlying idea is that if one shows contraction between two measures, then this implies a unique invariant measure and convergence towards it. The general setup of these results follow from

$$W_q(\nu_0 P_h^n, \nu) \leq \underbrace{W_q(\nu_0 P_h^n, \nu^\lambda)}_{\text{sampling error}} + \underbrace{W_q(\nu^\lambda, \nu)}_{\text{approxiamtion error}},$$

where  $\nu_0$  is some initial measure,  $P_h^n$  is a Markov transition kernel based on some algorithm with step-size  $h > 0$  after  $n$ -steps, and  $\nu$  is the target measure. Providing bounds of the form, translates to how many  $n$ -steps are required to achieve an accuracy of  $\varepsilon$ , for  $\varepsilon > 0$ . Below we provide the definition of the Wasserstein distance, which is required, before stating our first result which is a proposition.

**Definition 2.2** ( $q$ -Wasserstein distance). *Let us define  $\mathcal{P}_q(\mathbb{R}^{2p})$  to be the set of probability measures which have  $q$ -th moment for  $q \in [1, \infty)$  (i.e.  $\mathbb{E}(\|Z\|^q) < \infty$ ). Then the  $q$ -Wasserstein distance, between two measures  $\nu, \nu' \in \mathcal{P}_q(\mathbb{R}^{2p})$ , is defined as*

$$W_q(\nu, \nu') = \left( \inf_{\xi \in \Gamma(\nu, \nu')} \int_{\mathbb{R}^p \times \mathbb{R}^p} \|z_1 - z_2\|_2^q d\xi(z_1, z_2) \right)^{1/q}, \quad (2.3)$$

where  $\|\cdot\|_2$  is the norm we consider, and  $\Gamma(\nu, \nu')$  is the set of measures with respective marginals of  $\nu$  and  $\nu'$ , where the infimum is over all couplings  $\xi$ .

We now state our first result, which is an upper Wasserstein bound between our target measure  $\nu$  and its corresponding approximation  $\nu^\lambda$ , based on the splitting schemes we have discussed. Such a result demonstrates that  $W_q(\nu, \nu^\lambda) \rightarrow 0$  as  $\lambda \rightarrow 0$ .

**Proposition 2.1.** *Under Assumptions 2.1-2.3, for any  $q \geq 1$  and any  $\lambda$  satisfying*

$$0 < \lambda < \left( \frac{\sqrt{c_1} r}{p+q} \wedge \frac{\sqrt{c_1} r e^{\text{osc}_\kappa(f)}}{3\sqrt{\pi} \text{Vol}(\mathcal{K})^p} \right),$$

*it holds that*

$$W_q(\nu, \nu^\lambda) \leq C(p, q) \cdot \begin{cases} \lambda, & 1/p + 1/q > 1, \\ \lambda \log^{1/q}(\frac{1}{\lambda}), & 1/p + 1/q = 1, \\ \lambda^{1/p+1/q}, & 1/p + 1/q < 1 \end{cases}$$

where

$$C(p, q) = C_0 \left[ p \cdot \frac{e^{4 \operatorname{osc}_{\mathcal{K}}(f)}}{c_1^{1/2}} \cdot \left( \frac{\max(R, 1)}{\min(r, 1)} \right)^{(2p+1)} \right]^{1/p+1/q},$$

and  $C_0 > 0$  is a universal constant, and recalling  $\operatorname{osc}_{\mathcal{K}}(f)$  is defined in Subsection 1.5.

If we analyze Proposition 2.1 above, we have a phase transition of the Wasserstein bound, that depends on both the dimension  $p$  and the order  $q$ . The above result is very similar to that of [YY25a], with the modification being from the altered constant  $C(p, q)$ , and the tuning parameter  $\lambda > 0$ . We will use this proposition for our convergence analysis in Section 3.

**Remark 2.3.** Before we discuss our main results, we would like to refer to Table 1, which provides a complexity analysis of our different algorithms. By CLMC (PULMC) we refer to the OLD, which is discretized by the Euler-Maruyama scheme, and similarly for CKLMC using the KLD. Complexity results of both have been proven, and we state them in the table as a point of comparison with our proposed splitting schemes.

### 3 Main Results

In this section we provide our main results of the introduced constrained algorithms, from the previous section. In particular we will provide a series of convergence results based on the Wasserstein complexity defined in Subsection 2.3. This will be done for CUBU, CBAOAB, their SG versions and also the SG-CKLMC, which utilizes the Euler-Maruyama discretization of the KLD. Finally, we provide a complexity analysis, in terms of the number of iterations to acquire a certain level of accuracy for each algorithm. We begin by first discussing CUBU. All proofs will be deferred to the Appendix.

#### 3.1 Convergence Analysis of CUBU

**Theorem 3.1** (Convergence of CUBU). *Under Assumptions 2.1-2.5, set  $\gamma = 2$ . Suppose that  $\lambda$  is sufficiently small and satisfies*

$$0 < \lambda < \left( \frac{\sqrt{c_1} r}{p+2} \wedge \frac{\sqrt{c_1} r e^{\operatorname{osc}_{\mathcal{K}}(f)}}{3\sqrt{\pi} \operatorname{Vol}(\mathcal{K}) p} \right).$$

Then, for any sufficiently small step size  $h > 0$  and any  $p > 2$ , it holds that

$$W_2(\nu, \nu_n^{\text{UBU}}) \leq e^{-\frac{mhn}{3M^\lambda}} W_2(\nu, \nu_0^{\text{UBU}}) + \left( \frac{1}{\sqrt{M^\lambda}} + C_1 \frac{M_1^\lambda}{(M^\lambda)^2} \right) \kappa \sqrt{ph^2} + C(p, 2) \lambda^{\frac{1}{2} + \frac{1}{p}}.$$

Moreover, when the initial point  $\theta_0^{\text{UBU}} = \mathbf{0}$  and  $\mathbf{v}_0^{\text{UBU}} \sim \mathcal{N}_p(0, I_p)$ , it holds that

$$W_1(\nu, \nu_n^{\text{UBU}}) \leq e^{-\frac{mhn}{3M^\lambda}} \sqrt{\frac{p}{m}} + \left( \frac{1}{\sqrt{M^\lambda}} + C_1 \frac{M_1^\lambda}{(M^\lambda)^2} \right) \kappa \sqrt{ph^2} + C(p, 1) \lambda.$$

Here,  $\kappa = M^\lambda/m$ ,  $C_1 > 0$  is a universal constant specified in Theorem 2.1, and  $C(p, q)$  is defined in Proposition 2.1.

For both Gauge projection and Euclidean projection, we adopt  $M^\lambda = \mathcal{O}(1/\lambda^2)$ ,  $M_1^\lambda = \mathcal{O}(1/\lambda^2)$  corresponding to Example 2.3 and Example 2.4. The preceding theorem implies the following corollary.

**Corollary 3.1.** *Let error level  $\varepsilon \in (0, 1)$  be small.*

(a) *We set  $\lambda = \Theta(h^{\frac{4p}{3p+2}})$ , and choose  $h > 0$ , with  $n \in \mathbb{N}^+$ , such that*

$$h = \mathcal{O}\left(\varepsilon^{\frac{3p+2}{2p+4}}\right), \quad n = \tilde{\Omega}\left(\varepsilon^{-\frac{11p+2}{4+2p}}\right),$$

*then we have that  $W_2(\nu_n^{\text{CUBU}}, \nu) = \tilde{\mathcal{O}}(\varepsilon)$ .*

(b) We set  $\lambda = \Theta(h)$ , and choose  $h > 0$ , with  $n \in \mathbb{N}^+$ , such that

$$h = \mathcal{O}(\varepsilon), \quad n = \tilde{\Omega}(\varepsilon^{-3}),$$

then we have that  $W_1(\nu_n^{\text{CUBU}}, \nu) = \tilde{\mathcal{O}}(\varepsilon)$ .

The number of iterations required by the CUBU algorithm to achieve  $W_2(\nu, \nu_n^{\text{CUBU}}) \leq \varepsilon$  is of order  $\mathcal{O}(\varepsilon^{-\frac{11p+2}{4+2p}})$ . When  $p > 2$ , we note that  $\frac{11p+2}{2p+4} \geq 5.5 - \frac{10}{2p}$ . Moreover, the number of iterations required to achieve  $W_1(\nu, \nu_n^{\text{CUBU}}) \leq \varepsilon$  is of order  $\mathcal{O}(\varepsilon^{-3})$ . By direct comparison with other methods based on Euler–Maruyama discretization (see Table 1), we observe an improvement in iteration complexity.

### 3.1.1 Extension to SG-CUBU

Now we focus on the CUBU algorithm with gradients, referred to as SG-CUBU. In the following theorem, we quantify the Wasserstein-1 and Wasserstein-2 distances between the distribution of the output of the SG-CUBU algorithm and the target density  $\nu$ .

**Theorem 3.2.** *Under Assumptions 2.1-2.4 and Assumption 2.6, suppose that  $\lambda$  satisfies*

$$0 < \lambda < \left( \frac{\sqrt{c_1} r}{p+2} \wedge \frac{\sqrt{c_1} r e^{\text{osc}_K(f)}}{3\sqrt{\pi} \text{Vol}(K) p} \right).$$

Then, for any  $p > 2$ ,  $\gamma \geq \sqrt{8M^\lambda}$  and the step size

$$0 < h < \left( \frac{mM^\lambda}{4\gamma\sigma_2^2} \wedge \frac{1}{2\gamma} \right),$$

it holds that

$$\begin{aligned} W_2(\nu_n^{\text{SG-CUBU}}, \nu^\lambda) &\leq \left(1 - \frac{mh}{8\gamma}\right)^{n/2} W_2(\nu_0^{\text{SG-CUBU}}, \nu) + \frac{2\gamma\sqrt{h}}{m} \sqrt{\frac{\sigma_1^2 L^2}{\sqrt{M^\lambda}} \left( \frac{h^2(M^\lambda)^2 d}{m^2} + \frac{d}{m} \right)} \\ &\quad + \sqrt{d}(\sqrt{M^\lambda} + \gamma)h^2 + 2C(p, 2)\lambda^{1/p+1/2}. \end{aligned}$$

Moreover, when initialize the algorithm with  $\boldsymbol{\vartheta}_0^{\text{SG-CUBU}} = \mathbf{0}$ , and  $\mathbf{v}_0^{\text{SG-CUBU}} \sim \mathcal{N}_p(0, I_p)$ , it follows that

$$\begin{aligned} W_1(\nu_n^{\text{SG-CUBU}}, \nu) &\leq \left(1 - \frac{mh}{8\gamma}\right)^{n/2} \sqrt{\frac{p}{m}} + \frac{2\gamma\sqrt{h}}{m} \sqrt{\frac{\sigma_1^2 L^2}{\sqrt{M^\lambda}} \left( \frac{h^2(M^\lambda)^2 d}{m^2} + \frac{d}{m} \right)} \\ &\quad + \sqrt{d}(\sqrt{M^\lambda} + \gamma)h^2 + C(p, 1)\lambda. \end{aligned}$$

$M^\lambda = \mathcal{O}(1/\lambda^2)$  in the previously stated theorem, we obtain the following corollary.

**Corollary 3.2.** *Let the error level  $\varepsilon \in (0, 1)$  be small, and set  $\gamma = \sqrt{8M^\lambda}$ .*

(a) Choose  $\lambda = \Theta(h)$ , and set  $h > 0$ , the batch size and the number of iterations  $b, n \in \mathbb{N}^+$  such that

$$h = \mathcal{O}\left(\varepsilon^{\frac{2p}{p+2}}\right), \quad b = \Omega\left(\varepsilon^{-\frac{6p+4}{p+2}}\right), \quad n = \tilde{\Omega}\left(\varepsilon^{-\frac{4p}{p+2}}\right),$$

then we have that  $W_2(\nu_n^{\text{SG-CUBU}}, \nu) = \tilde{\mathcal{O}}(\varepsilon)$ .

(b) Set  $\lambda = \Theta(h)$ , and choose  $h > 0$ , with the batch size and the number of iterations  $b, n \in \mathbb{N}^+$ , such that

$$h = \mathcal{O}(\varepsilon), \quad b = \Omega(\varepsilon^{-4}), \quad n = \tilde{\Omega}(\varepsilon^{-2}),$$

then we have that  $W_1(\nu_n^{\text{SG-CUBU}}, \nu) = \tilde{\mathcal{O}}(\varepsilon)$ .

The number of gradient evaluations required by the SG-CUBU algorithm to achieve  $W_2(\nu, \nu_n^{\text{SG-CUBU}}) \leq \varepsilon$  is of order  $\mathcal{O}(\varepsilon^{-\frac{10p+4}{p+2}})$ . When  $p > 2$ , we note that  $\frac{10p+4}{p+2} \geq \frac{10p+20}{p+2} - \frac{16}{p+2}$ . Moreover, the number of gradient evaluations required to achieve  $W_1(\nu, \nu_n^{\text{SG-CUBU}}) \leq \varepsilon$  is of order  $\mathcal{O}(\varepsilon^{-6})$ .

### 3.2 Convergence Analysis of CBAOAB

Let us now extend our results and setup to the methodology of constrained BAOAB, i.e. CBAOAB. The following theorem presents the convergence results of the BAOAB scheme under constraints.

**Theorem 3.3.** *Under Assumptions 2.1-2.5, assume that  $\lambda$  satisfies*

$$0 < \lambda < \left( \frac{\sqrt{c_1} r}{p+2} \wedge \frac{\sqrt{c_1} r e^{\text{osc}_K(f)}}{3\sqrt{\pi} \text{Vol}(K) p} \right).$$

Then, for any  $p > 2$ ,  $\gamma \geq 2\sqrt{M^\lambda}$  and the step size  $h$  is chosen as

$$0 < h < \left( \frac{1 - e^{-\gamma h}}{4\sqrt{M^\lambda}} \wedge \frac{4\gamma}{m} \right),$$

it holds that

$$W_2(\nu_n^{\text{CBAOAB}}, \nu) \leq 21e^{-\frac{mh(n-1)}{4\gamma}} W_2(\nu_0^{\text{CBAOAB}}, \nu) + 66000 \frac{\sqrt{M^\lambda}}{m} \left( 4\sqrt{M^\lambda} p + \frac{3M_1^\lambda p}{M^\lambda} \right) \gamma h^2 + C(p, 2) \lambda^{1/2+1/p}.$$

Moreover, when the initial point  $\vartheta_0^{\text{CBAOAB}} = \mathbf{0}$  and  $\mathbf{v}_0^{\text{CBAOAB}} \sim \mathcal{N}_p(0, I_p)$ , it holds that

$$W_1(\nu_n^{\text{CBAOAB}}, \nu) \leq 21e^{-\frac{mh(n-1)}{4\gamma}} \sqrt{\frac{p}{m}} + 66000 \frac{\sqrt{M^\lambda}}{m} \left( 4\sqrt{M^\lambda} p + \frac{3M_1^\lambda p}{M^\lambda} \right) \gamma h^2 + C(p, 1) \lambda.$$

where  $C(p, 1)$  and  $C(p, 2)$  are given in Proposition 2.1.

Setting  $M_1^\lambda = \mathcal{O}(1/\lambda^2)$ ,  $M^\lambda = \mathcal{O}(1/\lambda^2)$  in the previously stated theorem, we obtain the following corollary.

**Corollary 3.3.** *Let the error level  $\varepsilon \in (0, 1)$  be small.*

(a) *Set  $\lambda = \Theta(h^{4p/(7p+2)})$ , and choose  $h > 0$  and the number of iterations  $n \in \mathbb{N}_+$  so that*

$$h = \mathcal{O}\left(\varepsilon^{\frac{7p+2}{2p+4}}\right), \quad n = \tilde{\Omega}\left(\varepsilon^{-\frac{11p-2}{2p+4}}\right),$$

*then we have  $W_2(\nu_n^{\text{CBAOAB}}, \nu) = \tilde{\mathcal{O}}(\varepsilon)$ .*

(b) *Set  $\lambda = \Theta(h^{1/2})$ , and choose  $h > 0$  and the number of iterations  $n \in \mathbb{N}_+$  so that*

$$h = \mathcal{O}(\varepsilon^2), \quad n = \tilde{\Omega}(\varepsilon^{-3}),$$

*then we have  $W_1(\nu_n^{\text{CBAOAB}}, \nu) = \tilde{\mathcal{O}}(\varepsilon)$ .*

A comparison between the iteration complexities of the CBAOAB method in this corollary and the CUBU method in Corollary 3.1 shows that they are of the same order, differing only by constant factors.

#### 3.2.1 Extension to SG-CBAOAB

As done before, we consider the additional extension of CBAOAB to that of stochastic gradients, which results in a new algorithm entitled SG-CBAOAB. Below we present a main convergence result and a corollary that details the computational complexity.

**Theorem 3.4.** *Under Assumptions 2.1-2.6, suppose that  $\lambda$  satisfies*

$$0 < \lambda < \left( \frac{\sqrt{c_1} r}{p+2} \wedge \frac{\sqrt{c_1} r e^{\text{osc}_K(f)}}{3\sqrt{\pi} \text{Vol}(K) p} \right).$$

Then, for any  $p > 2$ ,  $\gamma \geq \sqrt{8M^\lambda}$  and the step size

$$0 < h < \left( \frac{1 - e^{-\gamma h}}{2\sqrt{M^\lambda}} \wedge \frac{4\gamma}{m} \wedge 1 \wedge \frac{1}{4\gamma} \right),$$

it holds that

$$\begin{aligned} W_2(\nu_n^{\text{SG-CBAOAB}}, \nu^\lambda) &\leq \frac{4(1 - e^{-\gamma h})}{m} K_{\text{noise}}(h) + (1 - \rho(h))^n \left( W_2(\nu_0^{\text{SG-CBAOAB}}, \nu^\lambda) + C_{\text{bias}} h (1 - e^{-\gamma h}) \right) \\ &\quad + C_{\text{bias}} h (1 - e^{-\gamma h}) + 2C(p, 2) \lambda^{1/p+1/2}. \end{aligned}$$

Moreover, when initialize the algorithm with  $\vartheta_0^{\text{SG-CBAOAB}} = \mathbf{0}$ , and  $\mathbf{v}_0^{\text{SG-CBAOAB}} \sim \mathcal{N}_p(0, I_p)$ , it follows that

$$\begin{aligned} W_1(\nu_n^{\text{SG-CBAOAB}}, \nu^\lambda) &\leq \frac{4(1 - e^{-\gamma h})}{m} K_{\text{noise}}(h) + (1 - \rho(h))^n \left( \sqrt{\frac{p}{m}} + C_{\text{bias}} h (1 - e^{-\gamma h}) \right) \\ &\quad + C_{\text{bias}} h (1 - e^{-\gamma h}) + C(p, 1) \lambda. \end{aligned}$$

Here,  $\rho(h) = \frac{mh^2}{4(1 - e^{-\gamma h})}$ ,  $C_{\text{bias}}$  and  $K_{\text{noise}}$  are explicit constants that are provided in Proposition A.1.

**Corollary 3.4.** Let the error level  $\varepsilon \in (0, 1)$  be sufficiently small.

- (a) Set  $\lambda = \Theta\left(h^{\frac{4p}{7p+2}}\right)$ , and choose the step size  $h > 0$ , batch size  $b \in \mathbb{N}_+$ , and number of iterations  $n \in \mathbb{N}_+$  so that

$$h = \mathcal{O}\left(\varepsilon^{\frac{7p+2}{2p+4}}\right), \quad b = \Omega\left(\varepsilon^{-\frac{7p+2}{p+2}}\right), \quad n = \tilde{\Omega}\left(\varepsilon^{-\frac{11p+2}{2p+4}}\right).$$

Then we have  $W_2(\nu_n^{\text{SG-CBAOAB}}, \nu) = \mathcal{O}(\varepsilon)$ .

- (b) Set  $\lambda = \Theta(h^{1/2})$ , and choose the step size  $h > 0$ , batch size  $b \in \mathbb{N}_+$ , and number of iterations  $n \in \mathbb{N}_+$  so that

$$h = \mathcal{O}(\varepsilon^2), \quad b = \Omega(\varepsilon^{-4}), \quad n = \tilde{\Omega}(\varepsilon^{-3}).$$

Then we have  $W_1(\nu_n^{\text{SG-CBAOAB}}, \nu) = \mathcal{O}(\varepsilon)$ .

The conclusion from the following corollary, is that the number of gradient evaluations required to achieve  $W_2(\nu, \nu_n^{\text{SG-CBAOAB}}) \leq \varepsilon$  is of order  $\mathcal{O}(\varepsilon^{-\frac{25p+6}{2p+4}})$ . Similarly, the number of gradient evaluations required to achieve  $W_1(\nu, \nu_n^{\text{SG-CBAOAB}}) \leq \varepsilon$  is of order  $\mathcal{O}(\varepsilon^{-7})$ .

**Remark 3.5.** We remark that unlike the full-gradient case, the complexity results of SG-CBAOAB are worse than SG-CUBU. The slower convergence rate is mainly due to the additional B-step, which brings in extra stochastic-gradient error. This additional error term leads to a less favorable overall error bound, meaning that BAOAB with stochastic gradients needs more gradient evaluations than stochastic-gradient UBU to attain the same level of accuracy.

### 3.3 Results for SG-CKLMC

Thanks to our refined analysis of the distance between the smooth surrogate and the target distribution, we are able to derive a tighter upper bound on the convergence rate of CKLMC with stochastic gradients (referred to as SG-CKLMC), as stated in the following theorem.

**Theorem 3.6.** Under Assumptions 2.1–2.4 and Assumption 2.6 (i)–(ii), assume that  $\lambda$  satisfies

$$0 < \lambda < \left( \frac{\sqrt{c_1} r}{p+2} \wedge \frac{\sqrt{c_1} r e^{\text{osc}_\kappa(f)}}{3\sqrt{\pi} \text{Vol}(\mathcal{K}) p} \right).$$

Then, for any  $\gamma \geq \sqrt{m + M^\lambda}$ , and any step size  $h$  such that

$$0 < h < \min \left\{ \frac{\gamma\tau}{2K_1}, \frac{2}{\gamma\tau}, \frac{1}{10\gamma}, \frac{m}{4\gamma M^\lambda} \right\}.$$

It holds that

$$\begin{aligned} \mathbb{W}_2(\nu_n^{\text{SG-CKLMC}}, \nu) &\leq \left(1 - \frac{0.75mh}{\gamma}\right)^n \mathbb{W}_2(\nu_0^{\text{SG-CKLMC}}, \nu) + \frac{\sqrt{2}M^\lambda h \sqrt{p}}{m} + 2C(p, 2)\lambda^{1/2+1/p} \\ &\quad + \frac{8\sqrt{2}\sigma_1 L}{m\gamma} \sqrt{\frac{C_{\mathcal{V}}}{1-2\tau}}. \end{aligned}$$

Here, the constants  $\tau$  and  $K_1$  are defined by

$$\tau = \frac{1}{2} \min \left\{ \frac{1}{4}, \frac{m}{M^\lambda + \gamma^2/2} \right\}, \quad K_1 = \max \left\{ \frac{16((M^\lambda)^2 + 2\gamma(M^\lambda)^2 + \sigma_1^2 L^2)}{(1-2\tau)\gamma^2}, \frac{4M^\lambda + 2\gamma^2(1-\tau) + 8\gamma}{1-2\tau} \right\}.$$

The constant  $C_{\mathcal{V}}$  is given by

$$C_{\mathcal{V}} = \int_{\mathbb{R}^{2p}} \mathcal{V}(\boldsymbol{\vartheta}, \mathbf{v}) \mu_0(d\boldsymbol{\vartheta}, d\mathbf{v}) + \frac{4}{\tau} \left( p + \frac{mf(0)}{2M^\lambda + \gamma^2} \right),$$

where the Lyapunov function  $\mathcal{V}$  is defined as

$$\mathcal{V}(\boldsymbol{\vartheta}, \mathbf{v}) = U^\lambda(\boldsymbol{\vartheta}) + \frac{\gamma^2}{4} (\|\boldsymbol{\vartheta} + \gamma^{-1}\mathbf{v}\|^2 + \|\gamma^{-1}\mathbf{v}\|^2 - \tau\|\boldsymbol{\vartheta}\|^2).$$

Moreover, when the initial point  $\boldsymbol{\theta}_0^{\text{SG-CKLMC}} = \mathbf{0}$  and  $\mathbf{v}_0^{\text{SG-CKLMC}} \sim \mathcal{N}_p(0, I_p)$ , it holds that

$$\mathbb{W}_1(\nu_n^{\text{SG-CKLMC}}, \nu) \leq \left(1 - \frac{0.75mh}{\gamma}\right)^n \sqrt{\frac{p}{m}} + \frac{\sqrt{2}M^\lambda h \sqrt{p}}{m} + \frac{8\sqrt{2}\sigma_1 L}{m\gamma} \sqrt{\frac{C_{\mathcal{V}}}{1-2\tau}} + C(p, 1)\lambda.$$

Adopting  $M^\lambda = \mathcal{O}(1/\lambda^2)$  in the previously stated theorem, we obtain the following corollary.

**Corollary 3.5.** *Let the error level  $\varepsilon \in (0, 1)$  be small.*

(a) *Set  $\lambda = \Theta(h^{1/4})$ , and choose  $h > 0$ , the batch size and the number of iterations  $b, n \in \mathbb{N}_+$  so that*

$$h = \mathcal{O}\left(\varepsilon^{\frac{8p}{p+2}}\right), \quad b = \Omega\left(\varepsilon^{-\frac{8p}{p+2}}\right), \quad n = \tilde{\Omega}\left(\varepsilon^{-\frac{10p}{p+2}}\right),$$

*then we have  $\mathbb{W}_2(\nu_n^{\text{SG-CKLMC}}, \nu) = \tilde{\mathcal{O}}(\varepsilon)$  after  $nb$  stochastic gradient evaluations.*

(b) *Set  $\lambda = \Theta(h^{1/4})$ , and choose  $h > 0$ , the batch size and the number of iterations  $b, n \in \mathbb{N}_+$  so that*

$$h = \mathcal{O}\left(\varepsilon^4\right), \quad b = \Omega\left(\varepsilon^{-4}\right), \quad n = \tilde{\Omega}\left(\varepsilon^{-5}\right),$$

*then we have  $\mathbb{W}_1(\nu_n^{\text{SG-CKLMC}}, \nu) = \tilde{\mathcal{O}}(\varepsilon)$  after  $nb$  stochastic gradient evaluations.*

By direction comparison, with the results from Corollary 3.2, we notice the SG-CKLMC has worse complexity rate, especially related to  $b$ , where for SG-CUBU it is of order  $\mathcal{O}(1)$ . Therefore in both cases of full and stochastic gradients, the constrained splitting schemes offer favorable results.

**Remark 3.7.** *We would like to remark that despite the favorable complexity of our constrained splitting schemes, the constrained algorithm of the randomized midpoint method (RMM) performs better [YY25b]. This is because the RMM, in general, can be viewed to be optimal in the kinetic Langevin regime [CLW20, CLW23], which also extends to the constrained setting. This is expected due to its favorable complexity. However, our motivation from using the splitting methods, in particular UBU, over RMM is that (i) it attains a strong order of 2, which has proven useful in the context of unbiased estimation, (ii) it requires only one gradient evaluation per step, and finally (iii) has better dimension dependence, i.e.  $\mathcal{O}(p^{1/4})$ , compared to for RMM which has  $\mathcal{O}(p^{1/3})$ , for dimension  $p > 0$ . Therefore these reasons act as our motivation for our intended work and analysis.*

## 4 Numerical Experiments

In this section we provide numerical experiments comparing the algorithms discussed in Table 1, for constrained sampling problems. We consider three problems, where the first two will be on a simple sampling problem subject to simplex constraints, where our final experiment will include a Bayesian linear regression problem. Due to the difficulty of computing high-dimensional Wasserstein distances, we focus on a two-dimensional setting in this section to facilitate clearer presentation and easier visualization. As a result, we will consider a 2-dimensional normal distribution, and consider the particular choices of  $\mathcal{K}$  which we will impose on the target distribution  $\nu$ . After-which, we will a final example on Bayesian linear regression.

### 4.1 Circular Constraint

For our first numerical experiment, we consider uses a Euclidean ball centered at the origin, which we write as  $\mathcal{K} = \mathcal{B}_2(0, R)$ , with radius denoted by  $R$ . Here we specify our radius as  $R = 0.5$ , and we employ a Gauge projection, because of the structure of  $\mathcal{K}$ , as it is symmetric. We will run each algorithm for  $n = 1000$  iterations and present the how well each algorithm samples under  $\mathcal{K}$ . We will choose the stepsize sufficiently small, but not overly small which will be a choice of  $h = 0.1$ . We will also use 64 minibatches for each stochastic gradient algorithm introduced. This general setup will be considered for all future experiments. Our first set of simulations are provided in Figure 1, which present a comparison between the the algorithms with full gradients. Futhermore, Figure 2 is a comparison of the stochastic gradient methods.

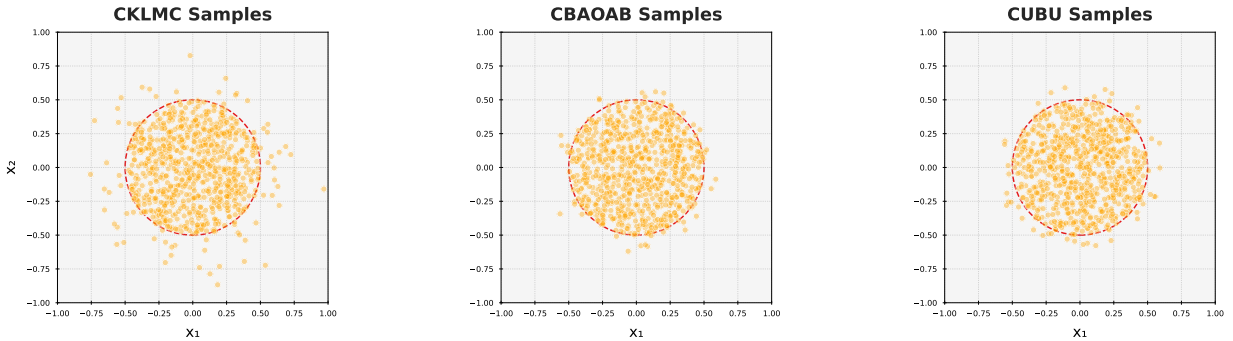


Figure 1: Comparison between different constraint algorithms, when aiming to sample from the circular convex set  $\mathcal{K}$  defined by  $\mathcal{K} = \mathcal{B}_2(0, R)$ . We consider  $n = 1000$  iterations and 2500 time steps.

Figure 1 and 2 demonstrates the sampling capabilities under the circular constraints. As we can see firstly from Figure 1, the sampling capability of CKLMC, which uses the Euler-Maruyama scheme, performs the worst, with many samples outside the convex set  $\mathcal{K}$ . However as we move towards the splitting schemes of CUBU, and CBAOAB we get a similar performance, in terms of the number of samples within the set. This is verifies the theoretical rates from Table 1. The extension to stochastic gradients is also considered in Figure 2, where we notice similar results as the full-gradient case.

### 4.2 Triangular Constraint

For our second numerical experiment, we now consider a modified constrained set which is a 3-simplex shifted away from the origin, of the form

$$\mathcal{K} = \left\{ (x_1, x_2) \in \mathbb{R}^2 : x_1, x_2 \geq -0.3, \quad x_1 + x_2 \leq 0.6 \right\} =: \Delta, \quad (4.1)$$

where again we apply the Gauge projection to enforce the constraint. As before we run each algorithm for  $n = 1000$  iterations and compare them under  $\mathcal{K}$ . Figure 3 below present such a comparison between

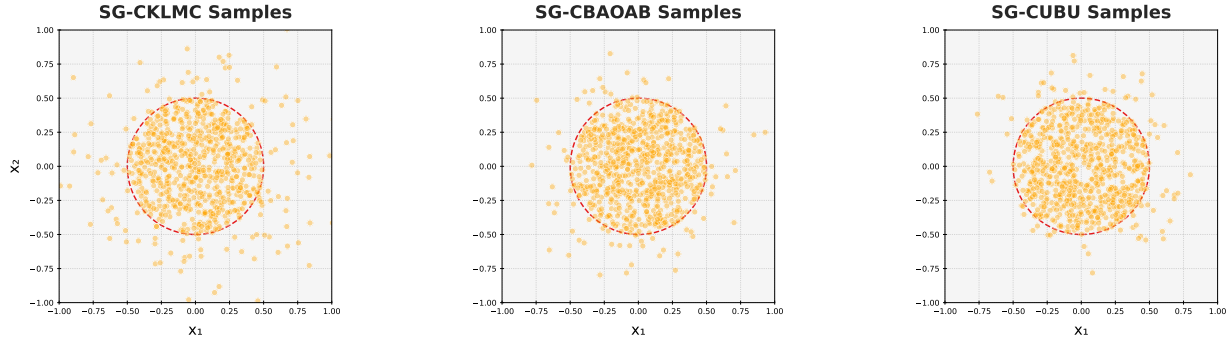


Figure 2: Comparison between different constraint algorithms with stochastic gradients, when aiming to sample from the circular convex set  $\mathcal{K}$  defined by  $\mathcal{K} = \mathcal{B}_2(0, R)$ . We consider  $n = 1000$  iterations and 2500 time steps.

the the algorithms with full gradients, and Figure 4 is a comparison of the stochastic gradient methods. By comparing the results, with the circular constraint, we see almost identical results which highlight the improved performance through the use of splitting schemes with full gradients, for the kinetic Langevin dynamics. Again, the same effect with stochastic gradients, where the splitting schemes perform better.

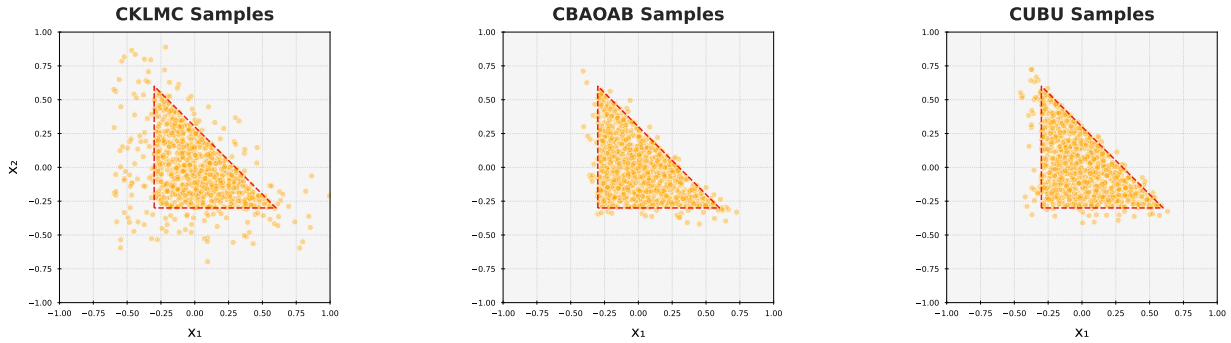


Figure 3: Comparison between different constraint algorithms, when aiming to sample from the triangular convex set  $\mathcal{K}$  defined in Eqn. (4.1). We consider  $n = 1000$  iterations and 2500 time steps.

### 4.3 Square Constraint

We now consider a final constrained on this problem, which is a square constraint. It will follow similarly to the triangular constraint, where now we define our set as

$$\mathcal{K} = \left\{ (x_1, x_2) \in \mathbb{R}^2 : -0.3 \leq x_1, x_2 \leq 0.6 \right\} =: \square, \quad (4.2)$$

where our results are presented in Figures 5 and 6. As expected, the constrained splitting schemes performing better compared to CKLMC and SG-CKLMC.

To summarize our first experiment, we provide a comparison of runtime, in seconds, between all the algorithms for the different choices of  $\mathcal{K}$ . This is presented through Table 2. As we expect the CKLMC is cheaper, however performs worse as demonstrated previously.

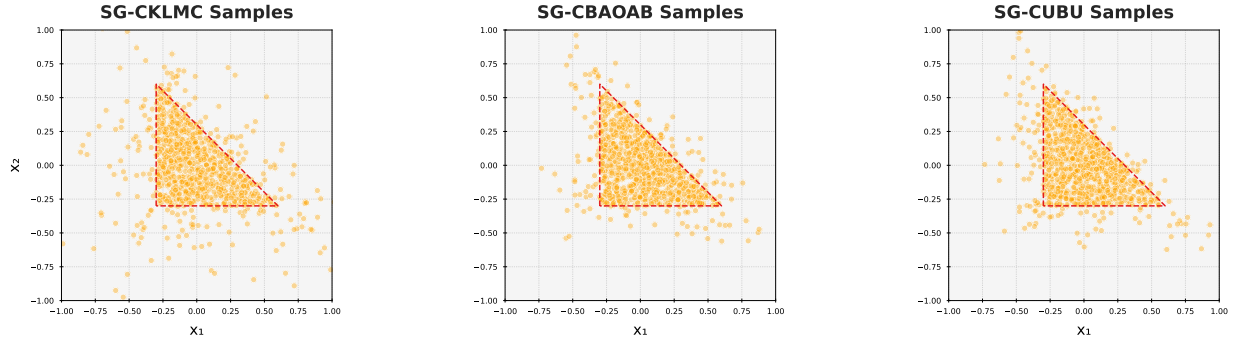


Figure 4: Comparison between different constraint algorithms with stochastic gradients, when aiming to sample from the triangular convex set  $\mathcal{K}$  defined in Eqn. (4.1). We consider  $n = 1000$  iterations and 2500 time steps.

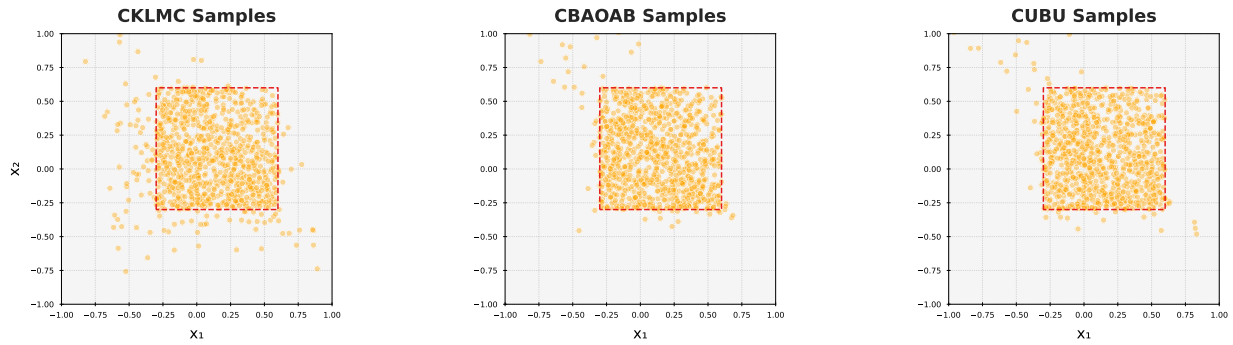


Figure 5: Comparison between different constraint algorithms, when aiming to sample from the square convex set  $\mathcal{K}$  defined in Eqn. (4.2). We consider  $n = 1000$  iterations and 2500 time steps.

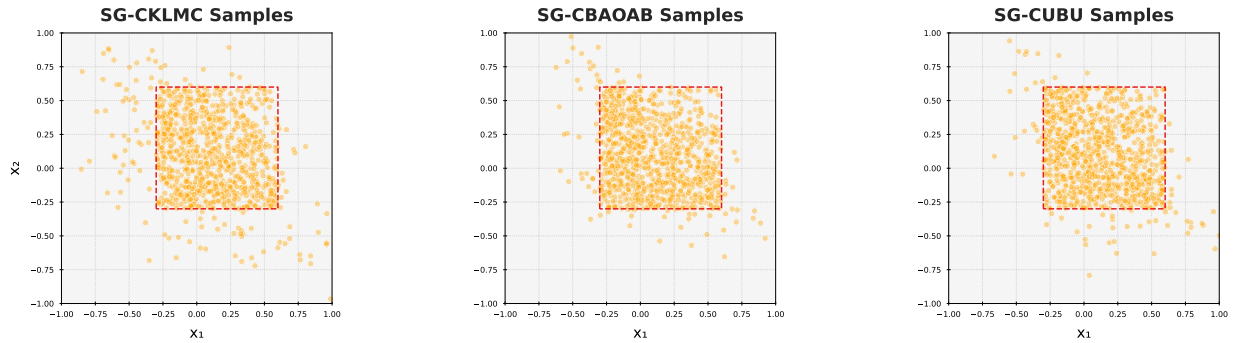


Figure 6: Comparison between different constraint algorithms with stochastic gradients, when aiming to sample from the square convex set  $\mathcal{K}$  defined in Eqn. (4.2). We consider  $n = 1000$  iterations and 2500 time steps.

#### 4.4 Bayesian Constrained Linear Regression

Our final numerical example we consider is a constrained version of Bayesian linear regression. Such examples exhibit applications in machine learning. An example of this is if the constraint set is an

| Algorithm | Runtime ( $\mathcal{K} = \mathcal{B}_2(0, R)$ ) | Runtime ( $\mathcal{K} = \triangle$ ) | Runtime ( $\mathcal{K} = \square$ ) |
|-----------|---|---------------------------------------|-------------------------------------|
| CKLMC     | 162.45 sec.                                     | 161.96 sec.                           | 162.39 sec.                         |
| CUBU      | 180.34 sec.                                     | 180.28 sec.                           | 181.63 sec.                         |
| CBAOAB    | 181.22 sec.                                     | 180.59 sec.                           | 180.97 sec.                         |
| SG-CKLMC  | 146.82 sec.                                     | 147.15 sec.                           | 147.03 sec.                         |
| SG-CUBU   | 163.72 sec.                                     | 164.05 sec.                           | 163.97 sec.                         |
| SG-CBAOAB | 163.85 sec.                                     | 164.19 sec.                           | 164.13 sec.                         |

Table 2: Comparison of the computational costs for constrained sampling problems, based on the different constrained set  $\mathcal{K}$ .

$\ell_p$ -ball around the origin, for  $p = 1$ , we obtain the Bayesian Lasso regression, and for  $p = 2$ , we get the Bayesian ridge regression. We will consider this for synthetic data. We will specifically consider the case when  $p = 1$ , which corresponds to the Bayesian Lasso regression, where we have a synthetic 2-dimensional problem. For our data we will generate  $n = 10,000$  data points  $(a_j, y_j)$  based on the following regression model

$$y_j = \boldsymbol{\theta}_*^\top a_j + \eta_j, \quad \eta_j \sim \mathcal{N}(0, 0.25), \quad (4.3)$$

where  $\boldsymbol{\theta}_* = [1, 1]^\top$  and  $a_j \sim \mathcal{N}(0, I)$ . We take the constraint set to be

$$\mathcal{C} = \{\boldsymbol{\theta} : \|\boldsymbol{\theta}\|_1 \leq 1\}.$$

Our prior distribution is chosen as the uniform distribution, where the constraints are satisfied. Finally, through Bayes' Theorem, the posterior distribution we have is

$$\pi(\boldsymbol{\theta}) = \frac{e^{\sum_{j=1}^{10,000} -\frac{1}{2}(y_j - x^\top a_j)^2} \cdot \mathbb{1}_{\mathcal{C}}}{\int_{\mathbb{R}^2} e^{\sum_{j=1}^{10,000} -\frac{1}{2}(y_j - x^\top a_j)^2} \cdot \mathbb{1}_{\mathcal{C}} d\boldsymbol{\theta}} \propto e^{\sum_{j=1}^{10,000} -\frac{1}{2}(y_j - x^\top a_j)^2} \cdot \mathbb{1}_{\mathcal{C}},$$

such that  $\mathbb{1}_{\mathcal{C}}$  is the indicator function for the constraint set  $\mathcal{C}$ . For this set of experiments, we take the batch size  $b = 50$  and run our algorithms with  $\eta = 0.001$ , the learning rate  $\delta = 10^{-5}$  where we reduce  $\delta$  by 15% every 2000 iterations. The total number of iterations is set to 8,000.

Our results of the simulations are presented in Figure 7 and Figure 8. In Figure 7 we present our results for constrained algorithms without stochastic gradients. As we can observe the worst performing algorithm is CKLMC, where most of the ‘‘mass’’ of the distribution is close to the yellow box, which is denoted by  $\boldsymbol{\theta}_* = [1, 1]^\top$ . However the distribution covers the full constrained set. This differs to the splitting schemes which perform better as much of the mass is based on the right boundary of the square, while the distribution not covering the full square. Figure 8 extends this to stochastic gradients where a similar phenomenon is observed as the previously conducted experiments.

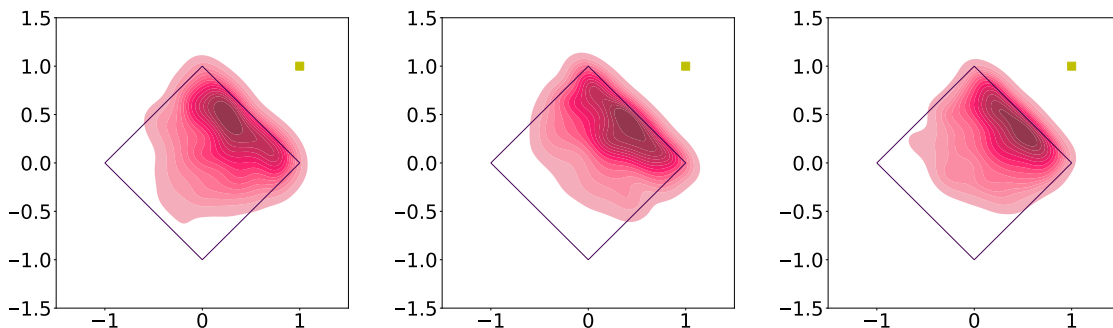


Figure 7: Experiments of the constrained Bayesian linear regression problem. Left figure: simulation using the CKLMC. Middle figure: CBAOAB. Right figure: CUBU. The constraint is yellow box.

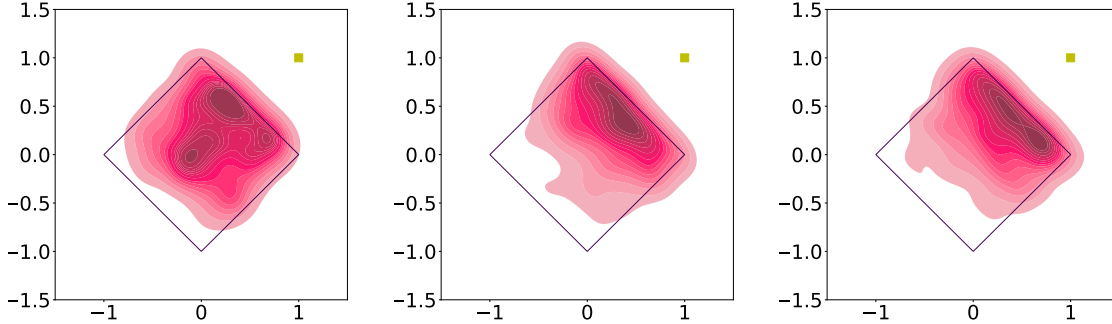


Figure 8: Experiments of the constrained Bayesian linear regression problem with stochastic gradients. Left figure: simulation using the SG-CKLMC. Middle figure: SG-CBAOAB. Right figure: SG-CUBU. The constraint is yellow box.

## 5 Conclusion

The purpose of this work was to provide new statistical algorithms for constrained sampling, based on the kinetic Langevin dynamics (KLD). In particular, we considered the use of splitting order schemes, that split the KLD into different components. This naturally promotes different splitting families, which include ABO and BU. We considered two such methods based on them, which are BAOAB and UBU, and its stochastic gradient (SG) versions. To consider a constrained setting, we provided a modified version of the potential function, and provided a convergence analysis in the Wasserstein metric. Furthermore, we were able to provide a complexity analysis in terms of the number of steps to achieve a certain level of accuracy. All our schemes demonstrate complexity gains over the KLD with the EM schemes, as shown in Table 1. Numerical evidence was provided that verified our theoretical findings. This includes a Bayesian linear regression problem.

There are a number of directions one can take with this work, related to constrained sampling.

- The first is the use of additional SG-splitting schemes, which have shown promise, such as the SMS-UBU method [PWCL25]. It is the first stochastic method able to attain a strong order of  $\mathcal{O}(h^2)$ , where it is based on applying minibatching without replacement, given through

$$\underbrace{(\mathcal{U}\mathcal{B}_{\omega_1}\mathcal{U})}_{\text{minibatch 1}} \dots \underbrace{(\mathcal{U}\mathcal{B}_{\omega_{N_m}}\mathcal{U})}_{\text{minibatch } N_m} \underbrace{(\mathcal{U}\mathcal{B}_{\omega_{N_m}}\mathcal{U})}_{\text{minibatch } N_m} \dots \underbrace{(\mathcal{U}\mathcal{B}_{\omega_1}\mathcal{U})}_{\text{minibatch 1}}, \mathcal{B}_{\omega_l}(x, v, h) = \left( x, v - hN_m \sum_{i \in \omega_l} \nabla f_i(x) \right),$$

and we have  $N_m := N_D/N_b$  minibatches.

- A second direction would be to consider alternative strategies for constrained sampling, for example confined sampling. In this setup one could consider reflected diffusion processes, such as the work of Leimkuhler et al. [LM, LST24]. Their setup is very different to ours, but allows a natural way to apply different splitting schemes, enabling new convergence and bias rates to be derived as well. The advantage of this approach, is that it does not have restrictions on the step-size. However the challenge is designing the constraints within the integrator's exponents.
- Finally, one could also apply such techniques in this paper to the application of unbiased estimation. Recent work has analyzed this for the KLD with splitting families which include a methodology entitled UBUBU [CLPW26, RCJ23]. Such a methodology is able to mitigate biases that arise, while being prevalent in high dimensions. To the best of our knowledge, the only work that has done unbiased constrained sampling is the work of Noble et al. [NBD24], however this requires the use of new sophisticated couplings. Ideas could also be utilized from [CLLW24].

## Acknowledgments

NKC is supported by an EPSRC-UKRI AI for Net Zero Grant: “Enabling CO2 Capture And Storage Projects Using AI”, (grant EP/Y006143/1). NKC is also supported by a City University of Hong Kong Start-up Grant, project number 7200809. LY is supported by the City University of Hong Kong Startup Grant and Hong Kong RGC Grant 21306325. NKC is also thankful to Peter Whalley for helpful comments.

## References

- [BDMP17] Nicolas Brosse, Alain Durmus, Eric Moulines, and Marcelo Pereyra. Sampling from a log-concave distribution with compact support with proximal langevin monte carlo. In *Conference on Learning Theory*, pages 319–342. PMLR, 2017.
- [CCBJ18] Xiang Cheng, Niladri S Chatterji, Peter L Bartlett, and Michael I Jordan. Underdamped Langevin MCMC: A non-asymptotic analysis. In *Conference on learning theory*, pages 300–323. PMLR, 2018.
- [CEAMR12] Gilles Celeux, Mohammed El Anbari, Jean-Michel Marin, and Christian P. Robert. Regularization in regression: comparing bayesian and frequentist methods in a poorly informative situation. *Bayesian Analysis*, 7(2):477–502, 2012.
- [Che25] Sinho Chewi. Log-concave sampling: Lecture notes. 2025.
- [CKK24] Luiz Chamon, Mohammad Reza Karimi, and Anna Korba. Constrained sampling with primal-dual langevin monte carlo. *Advances in Neural Information Processing Systems*, 2024.
- [CLLW24] Neil K Chada, Quanjun Lang, Fei Lu, and Xiong Wang. A data adaptive rkhs prior for bayesian learning of kernels in operators. *Journal of Machine Learning Research*, 25:1–37, 2024.
- [CLPW26] Neil K Chada, Benedict Leimkuhler, Daniel Paulin, and Peter A Whalley. Unbiased kinetic Langevin Monte Carlo with inexact gradients. *Annals of Statistics (to appear)*, 2026.
- [CLW20] Yu Cao, Jianfeng Lu, and Lihan Wang. Complexity of randomized algorithms for underdamped langevin dynamics. *arXiv preprint arXiv:2003.09906*, 2020.
- [CLW23] Yu Cao, Jianfeng Lu, and Lihan Wang. On explicit  $L^2$ -convergence rate estimate for underdamped Langevin dynamics. *Arch. Ration. Mech. Anal.*, 247(5):Paper No. 90, 34, 2023.
- [Dal17] Arnak S. Dalalyan. Theoretical guarantees for approximate sampling from smooth and log-concave densities. *J. R. Stat. Soc. Ser. B. Stat. Methodol.*, 79(3):651–676, 2017.
- [DFT<sup>+</sup>25] Hengrong Du, Qi Feng, Changwei Tu, Xiaoyu Wang, and Lingjiong Zhu. Non-reversible langevin algorithms for constrained sampling. *arXiv preprint arXiv:2501.11743*, 2025.
- [DRD20] Arnak S. Dalalyan and Lionel Riou-Durand. On sampling from a log-concave density using kinetic Langevin diffusions. *Bernoulli*, 26(3):1956–1988, 2020.
- [EGZ19] Andreas Eberle, Arnaud Guillin, and Raphael Zimmer. Couplings and quantitative contraction rates for Langevin dynamics. *Annals of Applied Probability*, 47(4):1982–2010, 2019.

- [GGZ22] Xuefeng Gao, Mert Gürbüzbalaban, and Lingjiong Zhu. Global convergence of stochastic gradient hamiltonian monte carlo for nonconvex stochastic optimization: Nonasymptotic performance bounds and momentum-based acceleration. *Operations Research*, 70(5):2931–2947, 2022.
- [Gho19] Hamid Ghorbani. Mahalanobis distance and its application for detecting multivariate outliers. *Facta Universitatis, Series: Mathematics and Informatics*, pages 583—595, 2019.
- [GHZ24] Mert Gurbuzbalaban, Yuanhan Hu, and Lingjiong Zhu. Penalized overdamped and underdamped langevin monte carlo algorithms for constrained sampling. *The Journal of Machine Learning Research*, 25(263):1–67, 2024.
- [HNPSD21] Jiri Hron, Roman Novak, Jeffrey Pennington, and Jascha Sohl-Dickstein. Wide bayesian neural networks have a simple weight posterior: theory and accelerated sampling. *In International Conference on Machine Learning*, 162:8926—8945, 2021.
- [KD24] S. Kandasamy and N. Dheeraj. The poisson midpoint method for langevin dynamics: provably efficient discretization for diffusion models. *Advances in Neural Information Processing Systems*, 2024.
- [KLV22] Yunbum Kook, Yin Tat Lee, and Santosh S. Vempala. Sampling with riemannian hamiltonian monte carlo in a constrained space. *Advances in Neural Information Processing Systems*, 2022.
- [LJ24] Gen Li and Yuchen Jiao. Improved convergence rate for diffusion probabilistic models. *arXiv preprint arXiv:2410.13738*, 2024.
- [LM] Benedict Leimkuhler and Charles Matthews. Efficient molecular dynamics using geodesic integration and solvent–solute splitting. *Proc. A*, 472(2189).
- [LM13] Benedict Leimkuhler and Charles Matthews. Robust and efficient configurational molecular sampling via Langevin dynamics. *Journal of Chemical Physics*, 138:174102, 2013.
- [LM15] Benedict Leimkuhler and Charles Matthews. Molecular dynamics. *Interdisciplinary applied mathematics*, 39:443, 2015.
- [LPW24a] Benedict Leimkuhler, Daniel Paulin, and Peter A Whalley. Contraction Rate Estimates of Stochastic Gradient Kinetic Langevin Integrators. *ESAIM: Mathematical Modelling and Numerical Analysis*, 58(6):2255–2286, 2024.
- [LPW24b] Benedict J. Leimkuhler, Daniel Paulin, and Peter A. Whalley. Contraction and Convergence Rates for Discretized Kinetic Langevin Dynamics. *SIAM Journal on Numerical Analysis*, 62(3):1226–1258, 2024.
- [LST24] Benedict Leimkuhler, Akash Sharma, and Michel Tretyakov. Numerical integrators for confined langevin dynamics. *arXiv preprint arXiv:2404.16584*, 2024.
- [NDBD24] M. Noble, V. De Bortoli, and A. O. Durmus. Unbiased constrained sampling with self-concordant barrier hamiltonian monte carlo. *Advances in Neural Information Processing Systems*, 2024.
- [PWCL25] Daniel Paulin, Peter A Whalley, Neil K Chada, and Benedict Leimkuhler. Sampling from bayesian neural network posteriors with symmetric minibatch splitting langevin dynamics. *AISTATS*, 2025.
- [RCJ23] Hamza Ruzayqat, Neil K. Chada, and Ajay Jasra. Unbiased estimation using underdamped Langevin dynamics. *SIAM J. Sci. Comput.*, 45(6):A3047–A3070, 2023.

- [SDWGM15] Jascha Sohl-Dickstein, Eric Weiss, Niru Maheswaranathan, and Surya Ganguli. Deep unsupervised learning using nonequilibrium thermodynamics. In *Proceedings of the 32nd International Conference on Machine Learning*, pages 2256–2265. PMLR, 2015.
- [SL19] Ruoqi Shen and Yin Tat Lee. The randomized midpoint method for log-concave sampling. *Advances in Neural Information Processing Systems*, 32, 2019.
- [SSDK21] Yang Song, Jascha Sohl-Dickstein, and Diederik P. et al. Kingma. Score-based generative modeling through stochastic differential equations. *ICLR*, 2021.
- [SSZ21] Jesus María Sanz-Serna and Konstantinos C. Zygalakis. Wasserstein distance estimates for the distributions of numerical approximations to ergodic stochastic differential equations. *J. Mach. Learn. Res.*, 22:Paper No. 242, 37, 2021.
- [Str63] Gilbert Strang. Accurate partial difference methods i: linear cauchy problems. *Archive for Rational Mechanics and Analysis*, 12(1):392–402, 1963.
- [XNZ08] Shiming Xiang, Feiping Nie, and Changshui Zhang. Learning a mahalanobis distance metric for data clustering and classification. In *International Conference on Machine Learning*, 12:3600—3612, 2008.
- [YY25a] Yifeng Yu and Lu Yu. Advancing wasserstein convergence analysis of score-based models: Insights from discretization and second-order acceleration. *arXiv preprint arXiv:2502.04849*, 2025.
- [YY25b] Yifeng Yu and Lu Yu. Randomized midpoint method for log-concave sampling under constraints. *Arxiv preprint*, 2025.
- [Zap21] Alfonso Alamo Zapatero. *Word Series for the Numerical Integration of Stochastic Differential Equations*. PhD thesis, Universidad de Valladolid, 2021.

## A Proofs of Theorems

The proofs of all our results, in the main text, are provided in this appendix. Specifically we will have our appendix divided into five sections, related to the each of the algorithms mentioned which are; (i) CUBU, (ii) SG-CUBU, (iii) CBAOAB, (iv) SG-CBAOAB and (v) SG-CKLMC. We discuss each in turn below.

### A.1 Proofs of convergence for CUBU

*Proof of Theorem 3.1.* By the triangle inequality, we have

$$W_2(\nu_n^{\text{CUBU}}, \nu) \leq W_2(\nu_n^{\text{CUBU}}, \nu^\lambda) + W_2(\nu^\lambda, \lambda).$$

The desired results follows readily from Proposition 2.1 and Theorem 2.1. Invoking the triangle inequality and the monotonicity of the Wasserstein distance, it holds that

$$W_1(\nu_n^{\text{CUBU}}, \nu) \leq W_1(\nu_n^{\text{CUBU}}, \nu^\lambda) + W_1(\nu^\lambda, \nu) \leq W_2(\nu_n^{\text{CUBU}}, \nu^\lambda) + W_1(\nu^\lambda, \nu).$$

Employing the results from Proposition 2.1 again gives the desired result.  $\square$

### A.2 Proofs of convergence for SG-CUBU

*Proof of Theorem 3.2.* Based on Theorem 15 from [PWCL25], when  $\gamma h < 1/2, \gamma \geq \sqrt{8M^\lambda}$ , we have

$$\begin{aligned} W_2(\nu_n^{\text{SG-CUBU}}, \nu^\lambda) &\leq \left(1 - \frac{mh}{4\gamma} + \frac{5h^2 C_G}{M^\lambda}\right)^{n/2} W_2(\nu_0^{\text{SG-CUBU}}, \nu^\lambda) \\ &\quad + \frac{\gamma\sqrt{M^\lambda}}{m - h\gamma C_G/M^\lambda} \frac{\sqrt{h}}{\sqrt{M^\lambda}} \sqrt{\frac{C_{SG}^2 L^2}{\sqrt{M^\lambda}} \left(\frac{h^2(M^\lambda)^2 d}{m^2} + \frac{d}{m}\right)} \\ &\quad + \sqrt{d}(\sqrt{M^\lambda} + \gamma)h^2. \end{aligned}$$

If  $h < \frac{mM^\lambda}{40\gamma C_G}$ , it holds that

$$\frac{h^2 C_G}{M^\lambda} < \frac{mh}{40\gamma},$$

which implies that

$$m - hC_G\gamma/M^\lambda > m/2,$$

that is

$$\frac{1}{m - \gamma h C_G / M^\lambda} < \frac{2}{m}.$$

Combining this with the previous display gives

$$\begin{aligned} W_2(\nu_n^{\text{SG-CUBU}}, \nu^\lambda) &\leq \left(1 - \frac{mh}{8\gamma}\right)^{n/2} W_2(\nu_0^{\text{SG-CUBU}}, \nu^\lambda) \\ &\quad + \frac{2\gamma\sqrt{h}}{m} \sqrt{\frac{C_{SG}^2 L^2}{\sqrt{M^\lambda}} \left(\frac{h^2(M^\lambda)^2 d}{m^2} + \frac{d}{m}\right)} \\ &\quad + \sqrt{d}(\sqrt{M^\lambda} + \gamma)h^2. \end{aligned}$$

Further simplification gives

$$\begin{aligned} W_2(\nu_n^{\text{SG-CUBU}}, \nu^\lambda) &\leq \left(1 - \frac{mh}{8\gamma}\right)^{n/2} W_2(\nu_0^{\text{SG-CUBU}}, \nu^\lambda) \\ &\quad + \frac{2C_{SG} L \gamma \sqrt{h}}{m} \sqrt{\frac{1}{\sqrt{M^\lambda}} \left(\frac{h^2(M^\lambda)^2 d}{m^2} + \frac{d}{m}\right)} \\ &\quad + \sqrt{d}(\sqrt{M^\lambda} + \gamma)h^2. \end{aligned}$$

Combining this with the result from Proposition 2.1 and using the triangle inequality gives the desired result.

The bound for the Wasserstein-1 distance follows a strategy similar to the proof of Theorem 3.1, relying on the monotonicity of the Wasserstein distance, the triangle inequality, and the results established in Proposition 2.1.  $\square$

### A.3 Proofs of convergence for CBAOAB

*Proof of Theorem 3.3.* By Theorem 5.1 and Theorem 8.5 in [LPW24b], when  $h < \frac{1-e^{-\gamma h}}{2\sqrt{M^\lambda}}$ , it follows from the triangle inequality that

$$\begin{aligned} W_2(\nu^\lambda, \nu_n^{\text{CBAOAB}}) &\leq W_2(\nu^\lambda, \nu_h^\lambda) + W_2(\nu_h^\lambda, \nu_n^{\text{CBAOAB}}) \\ &\leq 21 \left(1 - \frac{h^2 m}{4(1-e^{-\gamma h})}\right)^{n-1} W_2(\nu_0^{\text{CBAOAB}}, \nu^\lambda) + 22 W_2(\nu^\lambda, \nu_h^\lambda) \\ &\leq 21 \left(1 - \frac{h^2 m}{4(1-e^{-\gamma h})}\right)^{n-1} W_2(\nu_0^{\text{CBAOAB}}, \nu^\lambda) + 66000 \frac{\sqrt{M^\lambda}}{m} \left(4\sqrt{M^\lambda p} + \frac{3M_1^\lambda p}{M^\lambda}\right) h(1-e^{-\gamma h}). \end{aligned}$$

Note that  $1 - e^{-\gamma h} \leq \gamma h$ . When  $h < \frac{4\gamma}{m}$ , it holds that

$$\frac{h^2 m}{4(1-e^{-\gamma h})} \geq \frac{h^2 m}{4\gamma h} = \frac{hm}{4\gamma}.$$

It then follows that

$$1 - \frac{h^2 m}{4(1-e^{-\gamma h})} \leq 1 - \frac{hm}{4\gamma}.$$

Combining this with the previous display and Proposition 2.1 gives

$$\begin{aligned} W_2(\nu_n^{\text{CBAOAB}}, \nu) &\leq W_2(\nu_n^{\text{CBAOAB}}, \nu^\lambda) + W_2(\nu^\lambda, \nu) \\ &\leq 21 \left(1 - \frac{hm}{4\gamma}\right)^{n-1} W_2(\nu_0^{\text{CBAOAB}}, \nu) + 66000 \frac{\sqrt{M^\lambda}}{m} \left(4\sqrt{L^\lambda p} + \frac{3M_1^\lambda p}{M^\lambda}\right) h(1-e^{-\gamma h}) \\ &\quad + C_1 \lambda^{1/2+1/p} p \\ &\leq 21 e^{-\frac{mh(n-1)}{4\gamma}} W_2(\nu_0^{\text{CBAOAB}}, \nu) + 66000 \frac{\sqrt{M^\lambda}}{m} \left(4\sqrt{M^\lambda p} + \frac{3M_1^\lambda p}{M^\lambda}\right) \gamma h^2 + C_1 \lambda^{1/2+1/p} p, \end{aligned}$$

where  $C_1$  is a universal constant. By the triangle inequality and the monotonicity of the Wasserstein distance, it holds that

$$\begin{aligned} W_1(\nu_n^{\text{CBAOAB}}, \nu) &\leq W_2(\nu_n^{\text{CBAOAB}}, \nu^\lambda) + W_1(\nu^\lambda, \nu) \\ &\leq W_2(\nu_n^{\text{CBAOAB}}, \nu_h^\lambda) + W_2(\nu_h^\lambda, \nu^\lambda) + W_1(\nu^\lambda, \nu). \end{aligned}$$

When the initial point  $\theta_0^{\text{CBAOAB}}$  is set to be the minimizer of the function  $f$  and  $\mathbf{v}_0^{\text{CBAOAB}} \sim \mathcal{N}_p(0, I_p)$ , it holds that

$$W_2(\nu_n^{\text{CBAOAB}}, \nu_h^\lambda) \leq 21 e^{-\frac{mh(n-1)}{4\gamma}} \left( \sqrt{\frac{p}{m}} + W_2(\nu^\lambda, \nu_h^\lambda) \right).$$

Combining this with the previous display gives

$$W_1(\nu_n^{\text{CBAOAB}}, \nu) \leq 21 e^{-\frac{mh(n-1)}{4\gamma}} \sqrt{\frac{p}{m}} + 66000 \frac{\sqrt{M^\lambda}}{m} \left(4\sqrt{M^\lambda p} + \frac{3M_1^\lambda p}{M^\lambda}\right) \gamma h^2 + C_2 \lambda p^{1+1/p}.$$

$\square$

## A.4 Proofs of convergence for SG-CBAOAB

We first introduce the coupling used to compare one stochastic-gradient CBAOAB step with its full-gradient counterpart. For notational simplicity, throughout this section we omit the superscript SG-BAOAB whenever no ambiguity arises. We also use  $\mathbf{sg}$  to denote the stochastic gradient scheme, and  $\mathbf{fg}$  to denote the full gradient scheme.

Fix  $k \geq 0$ . Let  $Z_k^{\mathbf{sg}} = (\boldsymbol{\vartheta}_k^{\mathbf{sg}}, \mathbf{v}_k^{\mathbf{sg}})$  denote the current state of the stochastic-gradient CBAOAB chain, and define the field  $\mathcal{F}_k := \sigma(\boldsymbol{\vartheta}_k^{\mathbf{sg}}, \mathbf{v}_k^{\mathbf{sg}})$ . Starting from the same initial state  $Z_k^{\mathbf{sg}}$ , we couple one CBAOAB step using the full gradient with one CBAOAB step using the stochastic gradient, with the same Gaussian noise used in the O-step. Denote by  $P_h$  and  $Q_h$  the CBAOAB kernel with step size  $h$  using the full gradient and the stochastic gradient, respectively. Let

$$Y_{k+1} \sim P_h(Z_k^{\mathbf{sg}}, \cdot),$$

be the next state produced by one full-gradient CBAOAB step, and let

$$Z_{k+1}^{\mathbf{sg}} \sim Q_h(Z_k^{\mathbf{sg}}, \cdot),$$

be the next state produced by one stochastic-gradient BAOAB step. We then define the one-step discrepancy by

$$\Delta Z_{k+1} := Z_{k+1}^{\mathbf{sg}} - Y_{k+1} = (\Delta \boldsymbol{\vartheta}_{k+1}, \Delta \mathbf{v}_{k+1}).$$

**Lemma A.1.** *Let  $\Delta Z_k = Z_k^{\mathbf{sg}} - Z_k^{\mathbf{fg}}, \mathcal{F}_k := \sigma(\boldsymbol{\vartheta}_k^{\mathbf{sg}}, \mathbf{v}_k^{\mathbf{sg}})$ . When  $h < 1, \sqrt{M^\lambda}h < 1/2$ , it holds that*

$$\mathbb{E}[\|\Delta Z_{k+1}\|^2 | \mathcal{F}_k] \leq \sigma_1^2 (M^\lambda)^2 h^2 \left( C_1 (\|\boldsymbol{\vartheta}_k^{\mathbf{sg}}\|^2 + \|\mathbf{v}_k^{\mathbf{sg}}\|^2) + C_2 p \right),$$

where  $C_1 = 2 + \frac{1}{4}(M^\lambda)^2(1 + \sigma_1^2)$  and  $C_2 = \frac{1}{16}$ .

*Proof.* Let  $\pi_h$  denote the invariant measure of  $P_h$ . Define the hypothetical full gradient chain  $\nu_n^{\mathbf{fg}} = \nu Q_h^0 P_h^n$  and the true stochastic gradient chain  $\nu_n^{\mathbf{sg}} = \nu Q_h^n$ . By the triangle inequality, we obtain the following decomposition.

$$W_2(\nu_n^{\mathbf{sg}}, \nu^\lambda) \leq W_2(\nu_n^{\mathbf{sg}}, \nu_n^{\mathbf{fg}}) + W_2(\nu_n^{\mathbf{fg}}, \pi_h) + W_2(\pi_h, \nu^\lambda).$$

By Theorem 5.1 and Theorem 8.5 from [LPW24b], we have

$$W_2(\mu_n^{\mathbf{fg}}, \pi_h) \lesssim \left(1 - \frac{mh^2}{4(1 - e^{-\gamma h})}\right)^n W_2(\mu_0^{\mathbf{fg}}, \pi_h)$$

and

$$W_2(\pi_h, \nu^\lambda) \lesssim \frac{\sqrt{M^\lambda}}{m} (\sqrt{M^\lambda}p + \frac{M_1^\lambda}{M^\lambda}p)h(1 - e^{-\gamma h})$$

Our next goal is to establish the upper bound for  $W_2(\nu_n^{\mathbf{sg}}, \nu_n^{\mathbf{fg}})$ . Note that

$$\begin{aligned} W_2(\nu_n^{\mathbf{sg}}, \nu_n^{\mathbf{fg}}) &= W_2(\nu Q_h^n, \nu P_h^n) \\ &\leq W_2(\nu Q_h^{n-1} Q_h, \nu Q_h^{n-1} P_h) + W_2(\nu Q_h^{n-1} P_h, \nu P_h^{n-1} P_h) \\ &\leq W_2(\nu Q_h^{n-1} Q_h, \nu Q_h^{n-1} P_h) + \left(1 - \frac{mh^2}{4(1 - e^{-\gamma h})}\right) W_2(\nu Q_h^{n-1}, \nu P_h^{n-1}) \\ &= \left(1 - \frac{mh^2}{4(1 - e^{-\gamma h})}\right) W_2(\nu_{n-1}^{\mathbf{sg}}, \nu_{n-1}^{\mathbf{fg}}) + W_2(\nu Q_h^{n-1} Q_h, \nu Q_h^{n-1} P_h). \end{aligned} \quad (\text{A.1})$$

To this end, we aim to derive the one-step kernel perturbation bound for  $W_2(\nu Q_h^{n-1} Q_h, \nu Q_h^{n-1} P_h)$ . Given the  $k$ -th iterate of SG-CBAOAB algorithm  $(\mathbf{v}_k, \boldsymbol{\vartheta}_k)$ , we consider performing one CBAOAB update from this state using full gradients  $\nabla U^\lambda$  and also the stochastic gradients  $\tilde{\nabla} U^\lambda$ .

$$(B) \mathbf{v}_k^{(1),\text{fg}} = \mathbf{v}_k - \frac{h}{2} \nabla U^\lambda(\boldsymbol{\vartheta}_k) \text{ and } \mathbf{v}_k^{(1),\text{sg}} = \mathbf{v}_k - \frac{h}{2} \tilde{\nabla} U^\lambda(\boldsymbol{\vartheta}_k)$$

$$(A) \boldsymbol{\vartheta}_k^{(1),\text{fg}} = \boldsymbol{\vartheta}_k + \frac{h}{2} \mathbf{v}_k^{(1),\text{fg}} \text{ and } \boldsymbol{\vartheta}_k^{(1),\text{sg}} = \boldsymbol{\vartheta}_k + \frac{h}{2} \mathbf{v}_k^{(1),\text{sg}}$$

Sample  $\xi_k \sim \mathcal{N}(0_p, I_p)$

$$(O) \mathbf{v}_k^{(2),\text{fg}} = \eta \mathbf{v}_k^{(1),\text{fg}} + \sqrt{1 - \eta^2} \xi_k \text{ and } \mathbf{v}_k^{(2),\text{sg}} = \eta \mathbf{v}_k^{(1),\text{sg}} + \sqrt{1 - \eta^2} \xi_k$$

$$(A) \boldsymbol{\vartheta}_k^{(2),\text{fg}} = \boldsymbol{\vartheta}_k^{(1),\text{fg}} + \frac{h}{2} \mathbf{v}_k^{(2),\text{fg}} \text{ and } \boldsymbol{\vartheta}_k^{(2),\text{sg}} = \boldsymbol{\vartheta}_k^{(1),\text{sg}} + \frac{h}{2} \mathbf{v}_k^{(2),\text{sg}}$$

$$(B) \mathbf{v}_{k+1}^{\text{fg}} = \mathbf{v}_k^{(2),\text{fg}} - \frac{h}{2} \nabla U^\lambda(\boldsymbol{\vartheta}_k^{(2),\text{fg}}) \text{ and } \mathbf{v}_{k+1}^{\text{sg}} = \mathbf{v}_k^{(2),\text{sg}} - \frac{h}{2} \tilde{\nabla} U^\lambda(\boldsymbol{\vartheta}_k^{(2),\text{sg}})$$

$$\boldsymbol{\vartheta}_{k+1}^{\text{fg}} = \boldsymbol{\vartheta}_k^{(2),\text{fg}} \text{ and } \boldsymbol{\vartheta}_{k+1}^{\text{sg}} = \boldsymbol{\vartheta}_k^{(2),\text{sg}}$$

Assumption of the noisy gradient is given as

$$\mathbb{E}[\tilde{\nabla} U^\lambda(\boldsymbol{\vartheta}_k) | \boldsymbol{\vartheta}_k] = \nabla U^\lambda(\boldsymbol{\vartheta}_k),$$

and

$$\mathbb{E}[\|\tilde{\nabla} U^\lambda(\boldsymbol{\vartheta}_k) - \nabla U^\lambda(\boldsymbol{\vartheta}_k)\|^2 | \boldsymbol{\vartheta}_k] \leq \sigma_1^2 (M^\lambda)^2 \|\boldsymbol{\vartheta}_k\|^2.$$

Define  $\Delta \boldsymbol{\vartheta}_{k+1} = \boldsymbol{\vartheta}_{k+1}^{\text{sg}} - \boldsymbol{\vartheta}_{k+1}^{\text{fg}}$ ,  $\Delta \mathbf{v}_{k+1} = \mathbf{v}_{k+1}^{\text{sg}} - \mathbf{v}_{k+1}^{\text{fg}}$ . Please note that the cumulative difference contributed by each stage is given by the following expression.

$$(B) \Delta \mathbf{v}_B = \mathbf{v}_k^{(1),\text{fg}} - \mathbf{v}_k^{(1),\text{sg}} = \frac{h}{2} (\nabla U(\boldsymbol{\vartheta}_k) - \tilde{\nabla} U(\boldsymbol{\vartheta}_k))$$

$$(A) \Delta \boldsymbol{\vartheta}_A = \boldsymbol{\vartheta}_k^{(1),\text{fg}} - \boldsymbol{\vartheta}_k^{(1),\text{sg}} = \frac{h^2}{4} (\nabla U(\boldsymbol{\vartheta}_k) - \tilde{\nabla} U(\boldsymbol{\vartheta}_k))$$

$$(O) \Delta \mathbf{v}_O = \mathbf{v}_k^{(2),\text{fg}} - \mathbf{v}_k^{(2),\text{sg}} = e^{-\gamma h} \Delta \mathbf{v}_B = \frac{h e^{-\gamma h}}{2} (\nabla U(\boldsymbol{\vartheta}_k) - \tilde{\nabla} U(\boldsymbol{\vartheta}_k))$$

$$(A) \Delta \boldsymbol{\vartheta}_{A'} = \boldsymbol{\vartheta}_k^{(2),\text{fg}} - \boldsymbol{\vartheta}_k^{(2),\text{sg}} = \Delta \boldsymbol{\vartheta}_A + \frac{h}{2} \Delta \mathbf{v}_O = \frac{h^2}{4} (1 + e^{-\gamma h}) (\nabla U(\boldsymbol{\vartheta}_k) - \tilde{\nabla} U(\boldsymbol{\vartheta}_k))$$

Thus,

$$\Delta \boldsymbol{\vartheta}_{k+1} = \frac{h^2}{4} (1 + e^{-\gamma h}) (\nabla U(\boldsymbol{\vartheta}_k) - \tilde{\nabla} U(\boldsymbol{\vartheta}_k))$$

and

$$\begin{aligned} \Delta \mathbf{v}_{k+1} &= \Delta \mathbf{v}_O - \frac{h}{2} (\nabla U^\lambda(\boldsymbol{\vartheta}_k^{(2),\text{fg}}) - \tilde{\nabla} U^\lambda(\boldsymbol{\vartheta}_k^{(2),\text{sg}})) \\ &= \Delta \mathbf{v}_O - \frac{h}{2} (\nabla U^\lambda(\boldsymbol{\vartheta}_k^{(2),\text{fg}}) - \nabla U^\lambda(\boldsymbol{\vartheta}_k^{(2),\text{sg}})) \\ &\quad - \frac{h}{2} (\nabla U^\lambda(\boldsymbol{\vartheta}_k^{(2),\text{sg}}) - \tilde{\nabla} U^\lambda(\boldsymbol{\vartheta}_k^{(2),\text{sg}})) \end{aligned}$$

WLOG, assume the minimizer of  $U^\lambda$  is at the origin. Let  $\mathcal{F}_k := \sigma_1(\boldsymbol{\vartheta}_k, \mathbf{v}_k)$ . We then have

$$\mathbb{E}[\|\Delta \boldsymbol{\vartheta}_{k+1}\|^2 | \mathcal{F}_k] \leq \frac{h^4}{16} (1 + \eta)^2 \sigma_1^2 (M^\lambda)^2 \|\boldsymbol{\vartheta}_k\|^2$$

and

$$\begin{aligned} \mathbb{E}[\|\Delta \mathbf{v}_{k+1}\|^2 | \mathcal{F}_k] &\leq \frac{\eta^2 h^2}{4} \sigma_1^2 (M^\lambda)^2 \|\boldsymbol{\vartheta}_k\|^2 + \frac{(M^\lambda)^2 h^6}{64} (1 + \eta)^2 \sigma_1^2 (M^\lambda)^2 \|\boldsymbol{\vartheta}_k\|^2 \\ &\quad + \frac{h^2}{4} (M^\lambda)^2 \sigma_1^2 \mathbb{E}[\|\boldsymbol{\vartheta}_k^{(2),\text{sg}}\|^2 | \mathcal{F}_k]. \end{aligned} \tag{A.2}$$

Note that

$$\boldsymbol{\vartheta}_k^{(2),\text{sg}} = \boldsymbol{\vartheta}_k + \frac{h}{2}(1+\eta)\mathbf{v}_k - \frac{h^2}{4}(1+\eta)\nabla U(\boldsymbol{\vartheta}_k) - \frac{h^2}{4}(1+\eta)(\tilde{\nabla}U^\lambda(\boldsymbol{\vartheta}_k) - \nabla U(\boldsymbol{\vartheta}_k)) + \frac{h}{2}\sqrt{1-\eta^2}\xi_k,$$

which implies

$$\begin{aligned} \mathbb{E}[\|\boldsymbol{\vartheta}_k^{(2),\text{sg}}\|^2|\mathcal{F}_k] &\leq 3\|\boldsymbol{\vartheta}_k\|^2 + \frac{3h^2}{4}(1+\eta)^2\|\mathbf{v}_k\|^2 + \frac{3h^4}{16}(1+\eta)^2(M^\lambda)^2\|\boldsymbol{\vartheta}_k\|^2 \\ &\quad + \frac{h^4}{16}(1+\eta)^2(M^\lambda)^2\sigma_1^2\|\boldsymbol{\vartheta}_k\|^2 + \frac{h^2}{4}(1-\eta^2)p \\ &= \left(3 + \frac{h^4}{16}(1+\eta)^2(M^\lambda)^2(3+\sigma_1^2)\right)\|\boldsymbol{\vartheta}_k\|^2 + \frac{3h^4}{4}(1+\eta)^2\|\mathbf{v}_k\|^2 + \frac{h^2}{4}(1-\eta^2)p \end{aligned}$$

Combining this with display (A.2) gives

$$\begin{aligned} \mathbb{E}[\|\Delta\mathbf{v}_{k+1}\|^2|\mathcal{F}_k] &\leq \frac{\eta^2 h^2}{4}\sigma_1^2(M^\lambda)^2\|\boldsymbol{\vartheta}_k\|^2 + \frac{(M^\lambda)^2 h^6}{64}(1+\eta)^2\sigma_1^2(M^\lambda)^2\|\boldsymbol{\vartheta}_k\|^2 + \frac{h^2}{4}(M^\lambda)^2\sigma_1^2 \times \\ &\quad \left[ \left(3 + \frac{h^4}{16}(1+\eta)^2(M^\lambda)^2(3+\sigma_1^2)\right)\|\boldsymbol{\vartheta}_k\|^2 + \frac{3h^4}{4}(1+\eta)^2\|\mathbf{v}_k\|^2 + \frac{h^2}{4}(1-\eta^2)p \right] \\ &= \left(\frac{\eta^2 h^2}{4} + \frac{(M^\lambda)^2 h^6}{64}(1+\eta)^2 + \frac{h^2}{4}\left(3 + \frac{h^4}{16}(1+\eta)^2(M^\lambda)^2(3+\sigma_1^2)\right)\right)\sigma_1^2(M^\lambda)^2\|\boldsymbol{\vartheta}_k\|^2 \\ &\quad + \frac{3h^6}{16}(1+\eta)^2(M^\lambda)^2\sigma_1^2\|\boldsymbol{\vartheta}_k\|^2 + \frac{h^4}{16}(1-\eta^2)\sigma_1^2(M^\lambda)^2p. \end{aligned}$$

Let  $\Delta Z_k = Z_k^{\text{sg}} - Z_k^{\text{fg}}, \mathcal{F}_k := \sigma_1(\boldsymbol{\vartheta}_k^{\text{sg}}, \mathbf{v}_k^{\text{sg}})$ . When  $h < 1, \sqrt{M^\lambda}h < 1/2$ , it holds that

$$\mathbb{E}[\|\Delta Z_{k+1}\|^2|\mathcal{F}_k] \leq \sigma_1^2(M^\lambda)^2 h^2 \left( C_1(\|\boldsymbol{\vartheta}_k^{\text{sg}}\|^2 + \|\mathbf{v}_k^{\text{sg}}\|^2) + C_2 p \right),$$

where  $C_1 = 2 + \frac{1}{4}(M^\lambda)^2(1 + \sigma_1^2)$  and  $C_2 = \frac{1}{16}$ . □

We proceed to establish the bound for  $W_2(\nu_n^{\text{sg}}, \nu^\lambda)$ .

Set  $Z = (\boldsymbol{\vartheta}, \mathbf{v})$  and Lyapunov function

$$V(Z) := \|Z\|^2 = \|\boldsymbol{\vartheta}\|^2 + \|\mathbf{v}\|^2.$$

Assume the step size  $h > 0$  satisfies

$$h \leq 1, \quad \sqrt{M^\lambda}h \leq \frac{1}{4}, \quad \gamma h \leq 1.$$

Let  $P_h$  denote the CBAOAB Markov kernel with full gradient  $\nabla U^\lambda$  and friction  $\gamma$ , and let  $\pi_h$  be its invariant law.

1. **Wasserstein contraction.** For all probability measures  $\mu, \nu$  on  $\mathbb{R}^{2p}$ ,

$$W_2(\mu P_h, \nu P_h) \leq (1 - \rho(h)) W_2(\mu, \nu), \quad \rho(h) := \frac{mh^2}{4(1 - e^{-\gamma h})}. \quad (\text{A.3})$$

2. **Bias to the target.** Let  $\nu^\lambda$  denote the invariant law of the underdamped Langevin SDE with potential  $U^\lambda$ . Then

$$W_2(\pi_h, \nu^\lambda) \leq C_{\text{bias}} h(1 - e^{-\gamma h}), \quad (\text{A.4})$$

where

$$C_{\text{bias}} := \frac{\sqrt{M^\lambda}}{m} \left( \sqrt{M^\lambda p} + \frac{M_1^\lambda}{M^\lambda p} \right). \quad (\text{A.5})$$

3. **Kernel-level Lyapunov drift in  $V$ .** There exist explicit constants

$$\lambda_{\text{fg}} := \frac{1}{16} \min\{m, \gamma\}, \quad C_{\text{fg}} := \left(10 + 8\frac{M^\lambda}{m} + \frac{4(M_1^\lambda)^2}{m^2} + \frac{8}{\gamma}\right)p, \quad (\text{A.6})$$

such that for every deterministic  $z \in \mathbb{R}^{2p}$ , if  $Y^+ \sim P_h(z, \cdot)$  then

$$\mathbb{E}[V(Y^+) \mid Y^0 = z] \leq (1 - \lambda_{\text{fg}}h)V(z) + C_{\text{fg}}h. \quad (\text{A.7})$$

(A.3) and (A.4) follow from Wasserstein contraction and weak error bounds for CBAOAB, and (A.7) follows from a Lyapunov analysis of the underdamped Langevin SDE and the local error of the splitting scheme.

**Proposition A.1.** *Let Assumptions 2.4-2.5, and 2.6 hold.*

*Define the constants*

$$\rho(h) := \frac{mh^2}{4(1 - e^{-\gamma h})}, \quad (\text{A.8})$$

$$C_{\text{bias}} := \frac{\sqrt{M^\lambda}}{m} \left( \sqrt{M^\lambda p} + \frac{M_1^\lambda}{M^\lambda p} \right), \quad (\text{A.9})$$

$$C_V := 3 \left( 2 + \frac{1}{4}(M^\lambda)^2(1 + \sigma_1^2) \right), \quad D_V := \frac{1}{16}(1 - e^{-\gamma h}), \quad (\text{A.10})$$

and

$$\lambda_{\text{fg}} := \frac{1}{16} \min\{m, \gamma\}, \quad C_{\text{fg}} := \left(10 + 8\frac{M^\lambda}{m} + \frac{4(M_1^\lambda)^2}{m^2} + \frac{8}{\gamma}\right)p. \quad (\text{A.11})$$

Assume that the noise level  $\sigma_1^2$  satisfies the smallness condition

$$\sigma_1^2 \leq \frac{\lambda_{\text{fg}}^2}{20(M^\lambda)^2 C_V}. \quad (\text{A.12})$$

Define

$$\lambda_{\text{sg}} := \frac{1}{2} \lambda_{\text{fg}} = \frac{1}{32} \min\{m, \gamma\}, \quad (\text{A.13})$$

and the SG drift constant

$$C_{\text{sg}}(h) := 2C_{\text{fg}} + \frac{5\sigma_1^2(M^\lambda)^2 D_V p}{\lambda_{\text{fg}} h}. \quad (\text{A.14})$$

Then the SG-CBAOAB chain satisfies the Lyapunov bound

$$\sup_{k \geq 0} \mathbb{E}[\|Z_k^{\text{sg}}\|^2] \leq C_{\text{mom}}, \quad C_{\text{mom}} := \mathbb{E}[\|Z_0^{\text{sg}}\|^2] + \frac{C_{\text{sg}}(h)}{\lambda_{\text{sg}}}. \quad (\text{A.15})$$

Define

$$K_{\text{noise}}^2(h) := \sigma_1^2(M^\lambda)^2 (C_V C_{\text{mom}} + D_V p). \quad (\text{A.16})$$

Then, for every  $n \geq 0$ ,

$$\begin{aligned} W_2(\nu_n^{\text{sg}}, \nu^\lambda) &\leq \frac{4(1 - e^{-\gamma h})}{m} K_{\text{noise}}(h) \\ &+ (1 - \rho(h))^n \left( W_2(\nu_0^{\text{sg}}, \nu^\lambda) + C_{\text{bias}} h (1 - e^{-\gamma h}) \right) + C_{\text{bias}} h (1 - e^{-\gamma h}). \end{aligned} \quad (\text{A.17})$$

*Proof of Proposition A.1.* We proceed in several steps.

Invoking Lemma A.1, we have

$$\mathbb{E}[\|\Delta\boldsymbol{\vartheta}_{k+1}\|^2 \mid \mathcal{F}_k] \leq \frac{h^4}{16}(1 + e^{-\gamma h})^2 \sigma_1^2 (M^\lambda)^2 \|\boldsymbol{\vartheta}_k\|^2,$$

and

$$\mathbb{E}[\|\Delta\mathbf{v}_{k+1}\|^2 \mid \mathcal{F}_k] \leq \sigma_1^2 (M^\lambda)^2 h^2 \left( C_1 (\|\boldsymbol{\vartheta}_k\|^2 + \|\mathbf{v}_k\|^2) + C_2 p \right),$$

where

$$C_1 := 2 + \frac{1}{4} (M^\lambda)^2 (1 + \sigma_1^2), \quad C_2 := \frac{1}{16} (1 - e^{-\gamma h}).$$

Since  $(1 + e^{-\gamma h})^2 \leq 4$  and  $h \leq 1$ , we obtain

$$\mathbb{E}[\|\Delta\boldsymbol{\vartheta}_{k+1}\|^2 \mid \mathcal{F}_k] \leq \sigma_1^2 (M^\lambda)^2 h^2 \|\boldsymbol{\vartheta}_k\|^2.$$

Thus for  $V(z) = \|z\|^2$ ,

$$\begin{aligned} \mathbb{E}[V(\Delta Z_{k+1}) \mid \mathcal{F}_k] &= \mathbb{E}[\|\Delta\boldsymbol{\vartheta}_{k+1}\|^2 + \|\Delta\mathbf{v}_{k+1}\|^2 \mid \mathcal{F}_k] \\ &\leq \sigma_1^2 (M^\lambda)^2 h^2 \left( (C_1 + 1) \|\boldsymbol{\vartheta}_k\|^2 + C_1 \|\mathbf{v}_k\|^2 + C_2 p \right) \\ &\leq \sigma_1^2 (M^\lambda)^2 h^2 \left( C_V (\|\boldsymbol{\vartheta}_k\|^2 + \|\mathbf{v}_k\|^2) + D_V p \right), \end{aligned}$$

with

$$C_V := 3C_1 = 3 \left( 2 + \frac{1}{4} (M^\lambda)^2 (1 + \sigma_1^2) \right), \quad D_V := C_2 = \frac{1}{16} (1 - e^{-\gamma h}).$$

In other words,

$$\mathbb{E}[V(\Delta Z_{k+1}) \mid \mathcal{F}_k] \leq \sigma_1^2 (M^\lambda)^2 h^2 \left( C_V V(Z_k^{\text{sg}}) + D_V p \right). \quad (\text{A.18})$$

**Step 2: SG Lyapunov drift via kernel drift of  $P_h$ .** We have the decomposition

$$Z_{k+1}^{\text{sg}} = Y_{k+1} + \Delta Z_{k+1}.$$

By Young's inequality in  $\mathbb{R}^{2p}$ , for any  $\varepsilon > 0$ ,

$$\|Y_{k+1} + \Delta Z_{k+1}\|^2 \leq (1 + \varepsilon) \|Y_{k+1}\|^2 + \left(1 + \frac{1}{\varepsilon}\right) \|\Delta Z_{k+1}\|^2.$$

Taking conditional expectation given  $\mathcal{F}_k$  and using (A.7) with  $z = Z_k^{\text{sg}}$  and (A.18), we get

$$\begin{aligned} \mathbb{E}[V(Z_{k+1}^{\text{sg}}) \mid \mathcal{F}_k] &\leq (1 + \varepsilon) \left[ (1 - \lambda_{\text{fg}} h) V(Z_k^{\text{sg}}) + C_{\text{fg}} h \right] \\ &\quad + \left(1 + \frac{1}{\varepsilon}\right) \sigma_1^2 (M^\lambda)^2 h^2 \left( C_V V(Z_k^{\text{sg}}) + D_V p \right). \end{aligned}$$

Hence

$$\mathbb{E}[V(Z_{k+1}^{\text{sg}}) \mid \mathcal{F}_k] \leq A(\varepsilon, h) V(Z_k^{\text{sg}}) + B(\varepsilon, h), \quad (\text{A.19})$$

where

$$A(\varepsilon, h) := (1 + \varepsilon) (1 - \lambda_{\text{fg}} h) + \left(1 + \frac{1}{\varepsilon}\right) \sigma_1^2 (M^\lambda)^2 h^2 C_V,$$

$$B(\varepsilon, h) := (1 + \varepsilon) C_{\text{fg}} h + \left(1 + \frac{1}{\varepsilon}\right) \sigma_1^2 (M^\lambda)^2 h^2 D_V p.$$

We now choose

$$\varepsilon := \frac{\lambda_{\text{fg}} h}{4}.$$

For  $h$  small enough,  $\varepsilon \leq 1$  and thus  $(1 + \varepsilon) \leq 2$ . Moreover,

$$(1 + \varepsilon) (1 - \lambda_{\text{fg}} h) \leq 1 - \frac{3}{4} \lambda_{\text{fg}} h.$$

We also have

$$1 + \frac{1}{\varepsilon} = 1 + \frac{4}{\lambda_{\text{fg}}h} \leq \frac{5}{\lambda_{\text{fg}}h},$$

provided  $\lambda_{\text{fg}}h \leq 1$ .

Hence,

$$A(\varepsilon, h) \leq 1 - \frac{3}{4}\lambda_{\text{fg}}h + \frac{5\sigma_1^2(M^\lambda)^2h^2C_V}{\lambda_{\text{fg}}h}.$$

Impose the small noise condition (A.12):

$$\frac{5\sigma_1^2(M^\lambda)^2h^2C_V}{\lambda_{\text{fg}}h} \leq \frac{1}{4}\lambda_{\text{fg}}h,$$

which yields

$$A(\varepsilon, h) \leq 1 - \frac{1}{2}\lambda_{\text{fg}}h.$$

Define

$$\lambda_{\text{sg}} := \frac{1}{2}\lambda_{\text{fg}} = \frac{1}{32}\min\{m, \gamma\}.$$

Then,

$$\mathbb{E}[V(Z_{k+1}^{\text{sg}}) | \mathcal{F}_k] \leq (1 - \lambda_{\text{sg}}h)V(Z_k^{\text{sg}}) + C_{\text{sg}}(h)h, \quad (\text{A.20})$$

where

$$C_{\text{sg}}(h) := \frac{B(\varepsilon, h)}{h} \leq 2C_{\text{fg}} + \frac{5\sigma_1^2(M^\lambda)^2D_Vp}{\lambda_{\text{fg}}h}.$$

This gives displays (A.13)–(A.14).

**Step 3: Uniform SG moment bound.** Taking expectations in (A.20),

$$\mathbb{E}[V(Z_{k+1}^{\text{sg}})] \leq (1 - \lambda_{\text{sg}}h)\mathbb{E}[V(Z_k^{\text{sg}})] + C_{\text{sg}}(h)h.$$

Solving this linear recursion gives, for all  $k \geq 0$ ,

$$\mathbb{E}[V(Z_k^{\text{sg}})] \leq (1 - \lambda_{\text{sg}}h)^k\mathbb{E}[V(Z_0^{\text{sg}})] + \frac{C_{\text{sg}}(h)}{\lambda_{\text{sg}}}.$$

Therefore,

$$\sup_{k \geq 0} \mathbb{E}[V(Z_k^{\text{sg}})] \leq C_{\text{mom}} := \mathbb{E}[V(Z_0^{\text{sg}})] + \frac{C_{\text{sg}}(h)}{\lambda_{\text{sg}}}.$$

**Step 4: One-step kernel perturbation in  $W_2$ .** Let  $\mu$  be any probability measure on  $\mathbb{R}^{2p}$  and  $Z_0 \sim \mu$ . From Step 1 we can couple

$$Y_1 \sim P_h(Z_0, \cdot), \quad Z_1^{\text{sg}} \sim Q_h(Z_0, \cdot)$$

using the same Gaussian noise so that  $\Delta Z_1 := Z_1^{\text{sg}} - Y_1$  satisfies (A.18) with  $Z_k^{\text{sg}}$  replaced by  $Z_0$ . Then

$$W_2^2(\mu Q_h, \mu P_h) \leq \mathbb{E}[\|Z_1^{\text{sg}} - Y_1\|^2] = \mathbb{E}[V(\Delta Z_1)].$$

If we take  $\mu$  to be the law of  $Z_k^{\text{sg}}$ , then by (A.18) and the uniform moment bound,

$$\begin{aligned} \mathbb{E}[V(\Delta Z_1)] &\leq \sigma_1^2(M^\lambda)^2h^2 \left( C_V \sup_{j \geq 0} \mathbb{E}[V(Z_j^{\text{sg}})] + D_Vp \right) \\ &\leq \sigma_1^2(M^\lambda)^2h^2 \left( C_V C_{\text{mom}} + D_Vp \right). \end{aligned}$$

Define

$$K_{\text{noise}}^2(h) := \sigma_1^2(M^\lambda)^2 \left( C_V C_{\text{mom}} + D_Vp \right).$$

Then

$$W_2(\mu Q_h, \mu P_h) \leq K_{\text{noise}}(h)h. \quad (\text{A.21})$$

**Step 5: SG–FG chain distance.** Let

$$\nu_n^{\text{fg}} := \nu P_h^n, \quad \nu_n^{\text{sg}} := \nu Q_h^n,$$

and define  $E_n := W_2(\nu_n^{\text{sg}}, \nu_n^{\text{fg}})$ . Then

$$\begin{aligned} E_n &= W_2(\nu Q_h^n, \nu P_h^n) \\ &\leq W_2(\nu Q_h^{n-1} Q_h, \nu Q_h^{n-1} P_h) + W_2(\nu Q_h^{n-1} P_h, \nu P_h^{n-1} P_h) \\ &\leq W_2(\nu Q_h^{n-1} Q_h, \nu Q_h^{n-1} P_h) + (1 - \rho(h)) E_{n-1}, \end{aligned}$$

where we used the contraction (A.3) for the second term. Applying (A.21) with  $\mu = \nu Q_h^{n-1}$ , we obtain

$$E_n \leq K_{\text{noise}}(h)h + (1 - \rho(h))E_{n-1}, \quad E_0 = 0.$$

Solving this recursion yields

$$E_n \leq K_{\text{noise}}(h)h \sum_{j=0}^{n-1} (1 - \rho(h))^j \leq \frac{K_{\text{noise}}(h)h}{\rho(h)}.$$

With  $\rho(h)$  as in (A.8), this gives

$$W_2(\nu_n^{\text{sg}}, \nu_n^{\text{fg}}) \leq \frac{4(1 - e^{-\gamma h})}{m} K_{\text{noise}}(h).$$

**Step 6: Final bound to  $\nu^\lambda$ .** Finally, decompose

$$W_2(\nu_n^{\text{sg}}, \nu^\lambda) \leq W_2(\nu_n^{\text{sg}}, \nu_n^{\text{fg}}) + W_2(\nu_n^{\text{fg}}, \pi_h) + W_2(\pi_h, \nu^\lambda).$$

We have just shown

$$W_2(\nu_n^{\text{sg}}, \nu_n^{\text{fg}}) \leq \frac{4(1 - e^{-\gamma h})}{m} K_{\text{noise}}(h).$$

From (A.3) and the fact that  $\pi_h$  is invariant for  $P_h$ ,

$$W_2(\nu_n^{\text{fg}}, \pi_h) \leq (1 - \rho(h))^n W_2(\nu, \pi_h).$$

By the triangle inequality and (A.4),

$$W_2(\nu, \pi_h) \leq W_2(\nu, \nu^\lambda) + W_2(\nu^\lambda, \pi_h) \leq W_2(\nu, \nu^\lambda) + C_{\text{bias}}h(1 - e^{-\gamma h}).$$

Finally,  $W_2(\pi_h, \nu^\lambda) \leq C_{\text{bias}}h(1 - e^{-\gamma h})$  again by (A.4). Combining these bounds yields (A.17), which completes the proof.  $\square$

*Proof of Theorem 3.4.* The Proof of Theorem 3.4 follows directly from Proposition A.1, and using the triangle inequality which obtains the same constants from Proposition 2.1.  $\square$

## A.5 Proofs of convergence for SG-CKLMC

This appendix section is devoted to the proof of Theorem 3.6. The proof technique is similar to that in [GHZ24], but here we provide an explicit expression for the Wasserstein distance and combine it with our refined analysis of the distance between the surrogate distribution and the target distribution.

To prove Theorem 3.6, we first establish the following lemma, which provides an upper bound on the second moment of the  $n$ -th iterate  $\vartheta_n$  generated by the SG-CKLMC algorithm. For notational simplicity, throughout this section we omit the superscript SG-CKLMC whenever no ambiguity arises.

**Lemma A.2.** *Assume that the step size  $h$  satisfies*

$$h \leq \min \left\{ \frac{\gamma\tau}{2K_1}, \frac{2}{\gamma\tau}, \frac{1}{10\gamma} \right\},$$

where

$$\tau = \frac{1}{2} \min \left\{ \frac{1}{4}, \frac{m}{M^\lambda + \gamma^2/2} \right\}, \quad K_1 = \max \left\{ \frac{16((M^\lambda)^2 + 2\gamma(M^\lambda)^2 + \sigma_1^2 L^2)}{(1-2\tau)\gamma^2}, \frac{4M^\lambda + 2\gamma^2(1-\tau) + 8\gamma}{1-2\tau} \right\}.$$

Then the SG-CKLMC iterates  $\{\vartheta_n\}_{n \geq 0}$  satisfy the uniform second moment bound

$$\|\vartheta_n\|_{\mathbb{L}_2}^2 \leq \frac{8}{(1-2\tau)\gamma^2} C_{\mathcal{V}}, \quad n \geq 0,$$

where

$$C_{\mathcal{V}} = \int_{\mathbb{R}^{2p}} \mathcal{V}(\vartheta, \mathbf{v}) \mu_0(d\vartheta, d\mathbf{v}) + \frac{4}{\tau} \left( p + \frac{mf(0)}{2M^\lambda + \gamma^2} \right),$$

and the Lyapunov function  $\mathcal{V}$  is defined by

$$\mathcal{V}(\vartheta, \mathbf{v}) = U^\lambda(\vartheta) + \frac{\gamma^2}{4} (\|\vartheta + \gamma^{-1}\mathbf{v}\|^2 + \|\gamma^{-1}\mathbf{v}\|^2 - \tau\|\vartheta\|^2).$$

*Proof.* The proof follows the same steps as Proposition 2.22 in [GHZ24], relying on Lemma EC.5 in [GGZ22].  $\square$

We are now ready to prove Theorem 3.6.

*Proof of Theorem 3.6.* Let  $\vartheta_n, \mathbf{v}_n$  be the iterates of the CKLMC algorithm with a stochastic gradient. Let  $(\mathbf{L}_t, \mathbf{V}_t)$  be the kinetic Langevin diffusion, coupled with  $(\vartheta_n, \mathbf{v}_n)$  through the same Brownian motion  $(\mathbf{W}_t; t \geq 0)$  and starting from a random point  $(\mathbf{L}_0, \mathbf{V}_0) \propto \exp(-f(\mathbf{y}) + \frac{1}{2}\|\mathbf{w}\|_2^2)$  such that  $\mathbf{V}_0 = \mathbf{v}_0$ . This means that

$$\begin{aligned} \mathbf{v}_{n+1} &= e^{-\gamma h} \mathbf{v}_n - \frac{1 - e^{-\gamma h}}{\gamma} \nabla \tilde{U}^\lambda(\vartheta_n) + \sqrt{2\gamma} \xi_{n+1} \\ \vartheta_{n+1} &= \vartheta_n + \frac{1 - e^{-\gamma h}}{\gamma} \mathbf{v}_n - \frac{e^{-\gamma h} - 1 + \gamma h}{\gamma^2} \nabla \tilde{U}^\lambda(\vartheta_n) + \sqrt{2\gamma} \xi'_{n+1}. \end{aligned}$$

To proceed with the proof, we introduce an auxiliary process.

$$\begin{aligned} \tilde{\mathbf{v}}_{n+1} &= e^{-\gamma h} \mathbf{v}_n - \frac{1 - e^{-\gamma h}}{\gamma} \nabla U^\lambda(\vartheta_n) + \sqrt{2\gamma} \xi_{n+1} \\ \tilde{\vartheta}_{n+1} &= \vartheta_n + \frac{1 - e^{-\gamma h}}{\gamma} \mathbf{v}_n - \frac{e^{-\gamma h} - 1 + \gamma h}{\gamma^2} \nabla U^\lambda(\vartheta_n) + \sqrt{2\gamma} \xi'_{n+1}. \end{aligned}$$

We set  $\tilde{\mathbf{v}}_0 = \mathbf{v}_0$  and  $\tilde{\vartheta}_0 = \vartheta_0$ . Our goal will be to bound the term  $x_n$  defined by

$$x_n = \left\| \mathbf{C}^{-1} \begin{bmatrix} \mathbf{v}_n - \mathbf{V}_{nh} \\ \vartheta_n - \mathbf{L}_{nh} \end{bmatrix} \right\|_{\mathbb{L}_2} \quad \text{with} \quad \mathbf{C} = \frac{1}{\gamma} \begin{bmatrix} \mathbf{0}_{p \times p} & -\gamma \mathbf{I}_p \\ \mathbf{I}_p & \mathbf{I}_p \end{bmatrix}. \quad (\text{A.22})$$

where the  $\mathbb{L}_2$ -norm of a random vector  $X$  is defined as  $\mathbb{E}[\|X\|_2^2]$ . Applying the triangle inequality, we have

$$x_{n+1} \leq \left\| \mathbf{C}^{-1} \begin{bmatrix} \mathbf{v}_{n+1} - \tilde{\mathbf{v}}_{n+1} \\ \boldsymbol{\vartheta}_{n+1} - \tilde{\boldsymbol{\vartheta}}_{n+1} \end{bmatrix} \right\|_{\mathbb{L}_2} + \left\| \mathbf{C}^{-1} \begin{bmatrix} \tilde{\mathbf{v}}_{n+1} - \mathbf{V}_{(n+1)h} \\ \tilde{\boldsymbol{\vartheta}}_{n+1} - \mathbf{L}_{(n+1)h} \end{bmatrix} \right\|_{\mathbb{L}_2} \quad (\text{A.23})$$

By Lemma A.2 and  $\gamma h < 0.1$ , we have

$$\begin{aligned} \left\| \mathbf{C}^{-1} \begin{bmatrix} \mathbf{v}_{n+1} - \tilde{\mathbf{v}}_{n+1} \\ \boldsymbol{\vartheta}_{n+1} - \tilde{\boldsymbol{\vartheta}}_{n+1} \end{bmatrix} \right\|_{\mathbb{L}_2} &\leq 2\|\mathbf{v}_{n+1} - \tilde{\mathbf{v}}_{n+1}\|_{\mathbb{L}_2} + \gamma\|\boldsymbol{\vartheta}_{n+1} - \tilde{\boldsymbol{\vartheta}}_{n+1}\|_{\mathbb{L}_2} \\ &\leq 2.1h\sigma_1L\|\boldsymbol{\vartheta}_n\|_{\mathbb{L}_2} \\ &\leq 2.1h\sigma_1L\sqrt{\frac{8}{(1-2\tau)\gamma^2}}C_V. \end{aligned}$$

By Theorem 2 in [DRD20], we obtain

$$\left\| \mathbf{C}^{-1} \begin{bmatrix} \tilde{\mathbf{v}}_{n+1} - \mathbf{V}_{(n+1)h} \\ \tilde{\boldsymbol{\vartheta}}_{n+1} - \mathbf{L}_{(n+1)h} \end{bmatrix} \right\|_{\mathbb{L}_2} \leq \left(1 - \frac{0.75mh}{\gamma}\right) \left\| \mathbf{C}^{-1} \begin{bmatrix} \mathbf{v}_n - \mathbf{V}_{nh} \\ \boldsymbol{\vartheta}_n - \mathbf{L}_{nh} \end{bmatrix} \right\|_{\mathbb{L}_2} + 0.75M^\lambda h^2 \sqrt{p},$$

provided that  $h \leq \frac{m}{4\gamma M^\lambda}$  and  $\gamma \geq \sqrt{M^\lambda + m}$ . Combining these two displays with inequality (A.23) gives

$$x_{n+1} \leq \left(1 - \frac{0.75mh}{\gamma}\right)x_n + 0.75M^\lambda h^2 \sqrt{p} + 2.1h\sigma_1L\sqrt{\frac{8C_V}{(1-2\tau)\gamma^2}}.$$

It then follows by induction that

$$x_n \leq \left(1 - \frac{0.75mh}{\gamma}\right)^n x_0 + \frac{\gamma M^\lambda h \sqrt{p}}{m} + \frac{8\sigma_1L}{m} \sqrt{\frac{C_V}{1-2\tau}}.$$

Note that  $x_0 = \gamma W_2(\nu_0, \nu^\lambda)$  and  $W_2(\nu_n, \nu^\lambda) \leq \|\boldsymbol{\vartheta}_n - \mathbf{L}_{nh}\|_{\mathbb{L}_2} \leq \gamma^{-1} \sqrt{2}x_n$ . We then have

$$W_2(\nu_n, \nu^\lambda) \leq \left(1 - \frac{0.75mh}{\gamma}\right)^n W_2(\nu_0, \nu^\lambda) + \frac{\sqrt{2}M^\lambda h \sqrt{p}}{m} + \frac{8\sqrt{2}\sigma_1L}{m\gamma} \sqrt{\frac{C_V}{1-2\tau}}.$$

When  $p > 2$ , applying the triangle inequality and Proposition 2.1, we obtain

$$\begin{aligned} W_2(\nu_n, \nu) &\leq W_2(\nu_n, \nu^\lambda) + W_2(\nu, \nu^\lambda) \\ &\leq \left(1 - \frac{0.75mh}{\gamma}\right)^n W_2(\nu_0, \nu^\lambda) + \frac{\sqrt{2}M^\lambda h \sqrt{p}}{m} + \frac{8\sqrt{2}\sigma_1L}{m\gamma} \sqrt{\frac{C_V}{1-2\tau}} + C(p, 2)\lambda^{1/2+1/p} \\ &\leq \left(1 - \frac{0.75mh}{\gamma}\right)^n W_2(\nu_0, \nu) + \frac{\sqrt{2}M^\lambda h \sqrt{p}}{m} + \frac{8\sqrt{2}\sigma_1L}{m\gamma} \sqrt{\frac{C_V}{1-2\tau}} + 2C(p, 2)\lambda^{1/2+1/p} \end{aligned}$$

as desired.

The bound for the Wasserstein-1 distance follows a strategy similar to the proof of Theorem 3.1, relying on the monotonicity of the Wasserstein distance, the triangle inequality, and the results established in Proposition 2.1.  $\square$

## B Algorithms

---

### Algorithm 1 Stochastic Gradient Constrained UBU (SG-CUBU)

---

Initialize  $(\boldsymbol{\vartheta}_0, \mathbf{v}_0) \in \mathbb{R}^{2p}$ , stepsize  $h > 0$ , sample size  $K > 0$  and friction parameter  $\gamma > 0$ .  
**for**  $k = 1, 2, \dots, K$  **do**

Sample  $Z_k^\boldsymbol{\vartheta}, Z_k^\mathbf{v}, \tilde{Z}_k^\boldsymbol{\vartheta}, \tilde{Z}_k^\mathbf{v}$  according to

$$\begin{aligned} Z^\boldsymbol{\vartheta} &:= \sqrt{\frac{2}{\gamma}} \left( \mathcal{Z}^{(1)} \left( h/2, \xi^{(1)} \right) - \mathcal{Z}^{(2)} \left( h/2, \xi^{(1)}, \xi^{(2)} \right) \right), \\ Z^\mathbf{v} &:= \sqrt{2\gamma} \mathcal{Z}^{(2)} \left( h/2, \xi^{(1)}, \xi^{(2)} \right), \end{aligned} \tag{B.1}$$

(U)  $(\boldsymbol{\vartheta}, \mathbf{v}) \rightarrow (\boldsymbol{\vartheta}_{k-1} + \frac{1-\eta^{1/2}}{\gamma} \mathbf{v}_{k-1} + Z_k^\boldsymbol{\vartheta}, \eta^{1/2} \mathbf{v}_{k-1} + Z_k^\mathbf{v})$

Sample  $\omega_k \sim \rho$

(B)  $\mathbf{v} \rightarrow \mathbf{v} - h\mathcal{G}(x, \omega_k)$

(U)  $(\boldsymbol{\vartheta}_k, \mathbf{v}_k) \rightarrow (x + \frac{1-\eta^{1/2}}{\gamma} v + \tilde{Z}_k^\boldsymbol{\vartheta}, \eta^{1/2} \mathbf{v} + \tilde{Z}_k^\mathbf{v})$

**end for**

Output: Samples  $(\boldsymbol{\vartheta}_k)_{k=0}^K$ .

---



---

### Algorithm 2 Stochastic Gradient Constrained BAOAB (SG-CBAOAB)

---

- Initialize  $(\boldsymbol{\vartheta}_0, \mathbf{v}_0) \in \mathbb{R}^{2p}$ , stepsize  $h > 0$  and friction parameter  $\gamma > 0$ .

- Sample  $\omega_1 \sim \rho$

- $G_0 \rightarrow \mathcal{G}(\boldsymbol{\vartheta}_0, \omega_1)$

- **for**  $k = 1, 2, \dots, K$  **do**

(B)  $\mathbf{v} \rightarrow \mathbf{v}_{k-1} - \frac{h}{2} G_{k-1}$

(A)  $\boldsymbol{\vartheta} \rightarrow \boldsymbol{\vartheta}_{k-1} + \frac{h}{2} v$

Sample  $\xi_k \sim \mathcal{N}(0_p, I_p)$

(O)  $\mathbf{v} \rightarrow \eta \mathbf{v} + \sqrt{1 - \eta^2} \xi_k$

(A)  $\boldsymbol{\vartheta}_k \rightarrow \boldsymbol{\vartheta} + \frac{h}{2} v$

Sample  $\omega_{k+1} \sim \rho$

$G_k \rightarrow \mathcal{G}(\boldsymbol{\vartheta}_k, \omega_{k+1})$

(B)  $\mathbf{v}_k \rightarrow \mathbf{v} - \frac{h}{2} G_k$

- Output: Samples  $(\boldsymbol{\vartheta}_k)_{k=0}^K$ .

---



---

### Algorithm 3 Stochastic Gradient Euler-Maruyama (SG-CKLMC)

---

- Initialize  $(\boldsymbol{\vartheta}_0, \mathbf{v}_0) \in \mathbb{R}^{2p}$ , stepsize  $h > 0$  and friction parameter  $\gamma > 0$ .

- **for**  $k = 1, 2, \dots, K$  **do**

Sample  $\omega_k \sim \rho$

Sample  $\xi_k \sim \mathcal{N}(0_p, I_p)$

$\boldsymbol{\vartheta}_k \rightarrow \boldsymbol{\vartheta}_{k-1} + h \mathbf{v}_{k-1}$

$\mathbf{v}_k \rightarrow \mathbf{v}_{k-1} - h\mathcal{G}(\boldsymbol{\vartheta}_{k-1}, \omega_k) - h\gamma \mathbf{v}_{k-1} + \sqrt{2\gamma h} \xi_k$

- Output: Samples  $(\boldsymbol{\vartheta}_k)_{k=0}^K$ .

---